FERMILAB

Accelerator Issues of Project X

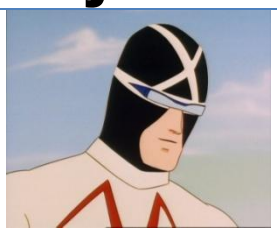

8/7/2007

Contributors

G. Apollinari
D. Bogert
A. Burov
J. Carneiro
B. Chase
C. Gattuso
P. Hurh
J. Hylen
D. Johnson
J. Johnstone
A. Klebaner
I. Kourbanis
J. Lackey
V. Lebedev
A. Leveling
M. Martens
S. Nagaitsev
E. Prebys
P. Ostroumov
A. Valishev
L. Vorobiev
R. Webber
D. Wildman,
R. Zwaska

Editor

D. McGinnis

1 Overview

1.1 Introduction

Project X is a concept for an intense 8 GeV proton source that provides beam for the Fermilab Main Injector and an 8 GeV physics program. The source consists of an 8 GeV superconducting linac that injects into the Recycler where multiple linac beam pulses are stripped and accumulated. The 8 GeV linac consists of a 1 GeV front end based on the design of the Proton Driver. The high energy end of the linac consists of ILC-like cryomodules. The use of the Recyler reduces the required charge in the superconducting 8 GeV linac to match the charge per pulse of the ILC design so that much of the ILC technology can be used in the design. This document is not meant to be a design report but is an overview of the basic concept and a discussion of the major accelerator physics issues that arise in this concept.

1.2 Motivation

The Fermilab Main Injector has the potential to provide intense energetic proton beams that can unlock discovery opportunities in neutrino physics and flavor physics. Currently, the relatively modern Main Injector is fed protons by an aged proton source. This source consists of a 400 MeV Linac followed by a rapid cycling 8 GeV Booster synchrotron. This source limits the Main Injector beam power to less than 700kW at 120 GeV. Future neutrino experiments will most likely require beam power exceeding 2MW at energies of 40 GeV and above. To provide this type of intense beam, the proton source must be capable of providing 400kW at the 8 GeV injection energy of the Main Injector. The current Fermilab proton source provides on the order of 30kW for the current neutrino program and has the capability of providing up to 70kW.

Space charge tune shift at injection into the Booster limits the beam power in the current Fermilab proton source. If the rapid cycling synchrotron is replaced with a linac, then space charge issues that plague the current Booster are almost completely mitigated. This is one of the chief motivations of the Fermilab Proton Driver design. The major issue of an 8 GeV injector linac is cost. Traditionally, the economic crossover energy at which a synchrotron becomes more cost-effective than a normal conducting linac has been in the range 0.1 ~ 0.5 GeV. As argued in the Proton Driver Design Report[1], the economic cross-over point is raised to the few GeV range with the advent of superconducting RF technology.

The superconducting 8 GeV linac described in the Proton Driver Design Report merges design concepts and technology from the ILC, the Spallation Neutron Source (SNS), the Rare Isotope Accelerator (RIA), JPARC, and other SCRF projects. The last two thirds of the linac consists of ILC type cryomodules and cavities operating at 1300 MHz. The front end of the linac consists mostly of spoke resonators operating at 325 MHz which is ¼ of the ILC frequency.

In the Proton Driver design, the beam from the H- linac injects directly into the Main Injector where the H- ions are stripped and captured in 53 MHz RF buckets. The 53 MHz bunches are pre-formed in the linac with a fast chopper. To provide 2MW of beam power at 120 GeV for a 1.4 second Main Injector ramp, the total charge injected into the Main Injector must be greater than 1.45×10^{14} protons. Since the beam is stripped in the Main Injector, the 8 GeV linac has to fill the Main Injector in a single pulse. If the pulse length is 1 ms (nominal ILC pulse length), the 8 GeV linac has to support an average current of 23mA over the 1mS pulse.

One of the key features of the superconducting 8 GeV linac is the synergy it shares with the ILC design. However, since the average beam current in the ILC design is 9 mA over a beam pulse length of 1 mS, the required charge per pulse in the Proton Driver design is a factor of 2.6 times larger than the nominal ILC charge per pulse. Because of this substantial difference in the charge per pulse, the design of the cryo-modules, the RF distribution system, and the cryogenic system could be significantly different between the ILC and the high energy end of the superconducting 8 GeV linac. For example, the ILC design calls for one klystron every three cryomodules. For the high energy end of the superconducting 8 GeV linac, the Proton Driver design would then require one klystron for every cryomodule. Or, if the average beam current in the superconducting 8 GeV linac is reduced to the ILC design current of 9 mA, the RF distribution in the high energy end of the superconducting 8 GeV linac could be the same as the ILC but the beam pulse length would be a factor of 2.6 times longer than the nominal ILC pulse.

It is desirable to have the ILC and the high energy end of the superconducting 8 GeV Linac designs to be as similar as possible. Synergy in the designs would help in both directions. First, the superconducting 8 GeV linac would benefit from the enormous engineering effort being expended on the design of the ILC main linac. In addition, cost savings resulting from industrialization, technological advances, etc. developed for the ILC would naturally be taken advantage of in the superconducting 8 GeV linac design.

In the other direction, ILC industrialization would benefit greatly from the construction of a superconducting 8 GeV linac. The ILC industrialization profile outlined in the RDR calls for each region to double production capacity over a four year program ending with a capacity to produce 25 cryomodules per year at the end of the fourth year. After four years, each region would have produced over 45 cryomodules. The high energy end of the superconducting 8 GeV linac requires about forty ILC-like cryo-modules. Thus, construction of the superconducting 8 GeV linac could serve as the impetus for ILC industrialization with the added bonus of providing a strong physics program with real discovery potential.

1.3 Concept

Because of the relatively long Main Injector ramp, the Proton Driver design can be modified so that the charge per pulse propagated though the superconducting 8 GeV linac matches the charge per pulse of the ILC. In the original Proton Driver design, the 8 GeV Linac fills the Main Injector in a single pulse and then remains idle during the Main Injector ramp cycle. The duration of the Main Injector ramp is about 1.4 seconds to reach an energy of 120 GeV. If the 8 GeV linac operates at the same cycle rate as the ILC design of 5 Hz, then the 8 GeV linac can support seven pulses during the Main Injector ramp.

As an alternative to the original Proton Driver design, a number of these beam pulses from the 8 GeV linac could instead be directed into the Recycler ring where each pulse is stripped and accumulated while the Main Injector is ramping. After the Main Injector ramp returns to the injection energy, the beam accumulated in the Recycler can be transferred into the Main Injector. Because the Main Injector and the Recycler have the same circumference, the beam can be transferred in a single turn. Using three of 8 GeV linac pulses to fill the Recycler would reduce the required charge per linac pulse needed for 2MW at 120 GeV to below the design value of the ILC charge per pulse. A schematic of the concept is shown in Figure 1.1.

Another very attractive feature of the 8 GeV linac is the large amount of 8 GeV beam power available as compared to an 8 GeV synchrotron. If the 8 GeV linac is designed for 9 mA of average beam current over a 1mS beam pulse length, with a cycle rate of 5 Hz (ILC parameters),

the 8 GeV linac can provide 360kW flux of protons at 8 GeV. Figure 1.2 shows the proton flux capability of the 8 GeV linac compared to present performance and other possible Fermilab proton source upgrades. Because a 120 GeV Main Injector cycle only needs three of the seven available 8 GeV linac pulses to provide over 2 MW at 120 GeV, the other four linac pulses can be used to provide beam to other 8 GeV physics programs. To provide beam to these other programs, an additional extraction system separate from the single turn extraction system used to feed the Main Injector would be required in the Recycler.

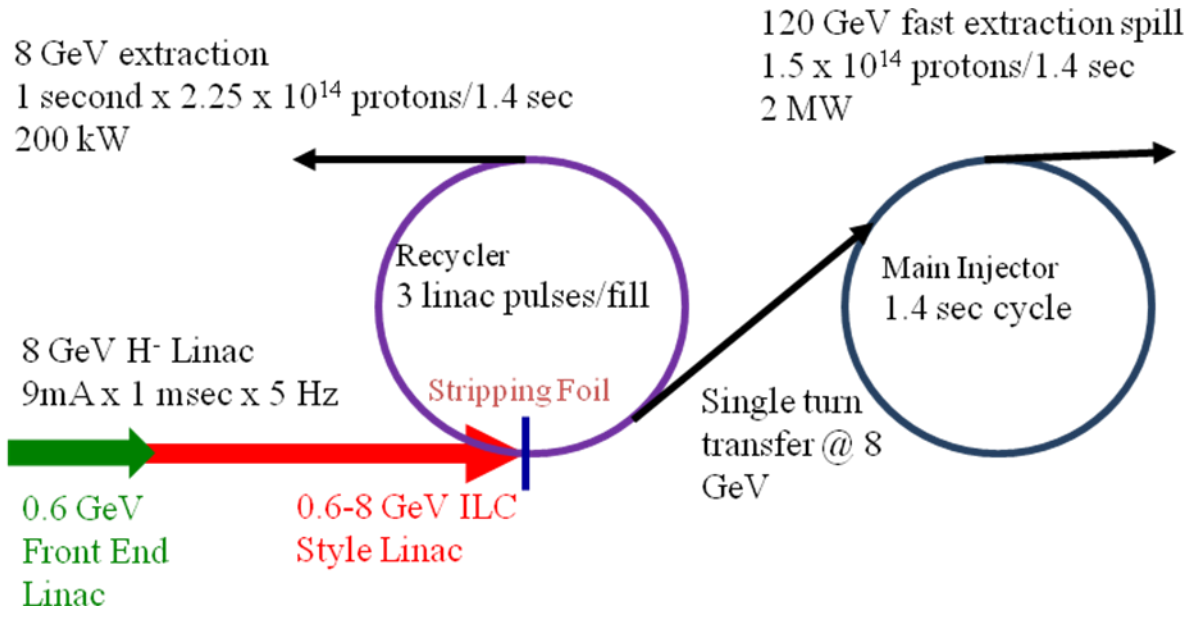

Figure 1.1 Schematic of an 8 GeV Linac and a Proton Accumulator

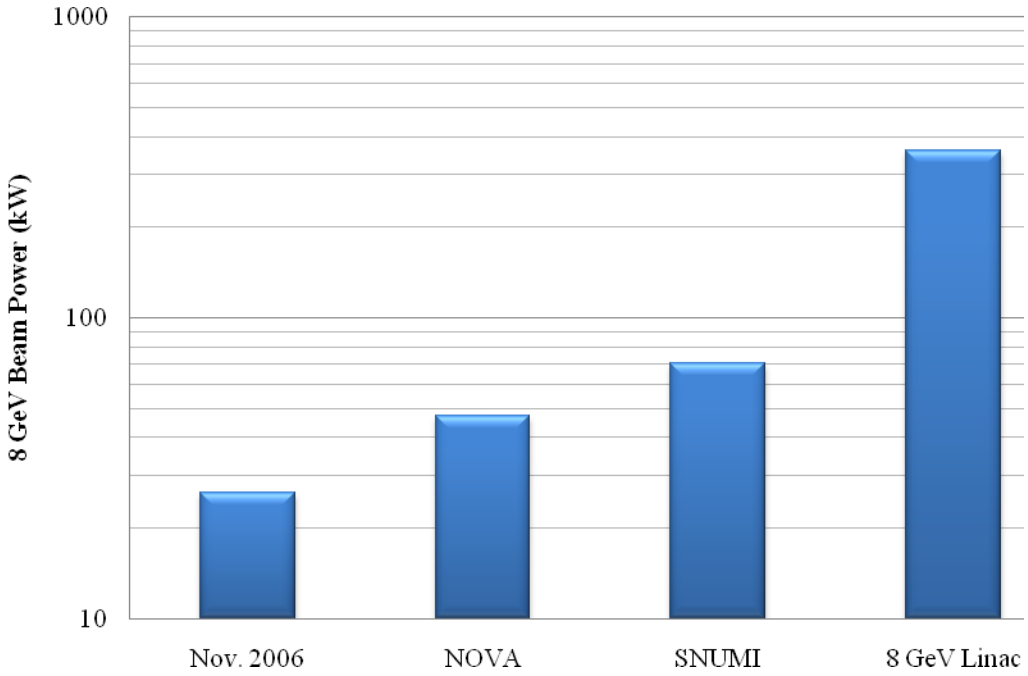

Figure 1.2 8 GeV Proton flux for various proton sources

The Main Injector can also be used to provide beam at a range of extraction energies if the physics program requires it. Neglecting the effects of the injection and extraction energy ramp parabolas, the Main Injector ramp length varies approximately linearly with extraction energy. For ILC parameters in beam current, pulse length, and cycle rate, the 8 GeV linac can supply enough protons for the Main Injector to reach over 2 MW at extraction energies of 50 GeV or greater as shown in Figure 1.3.

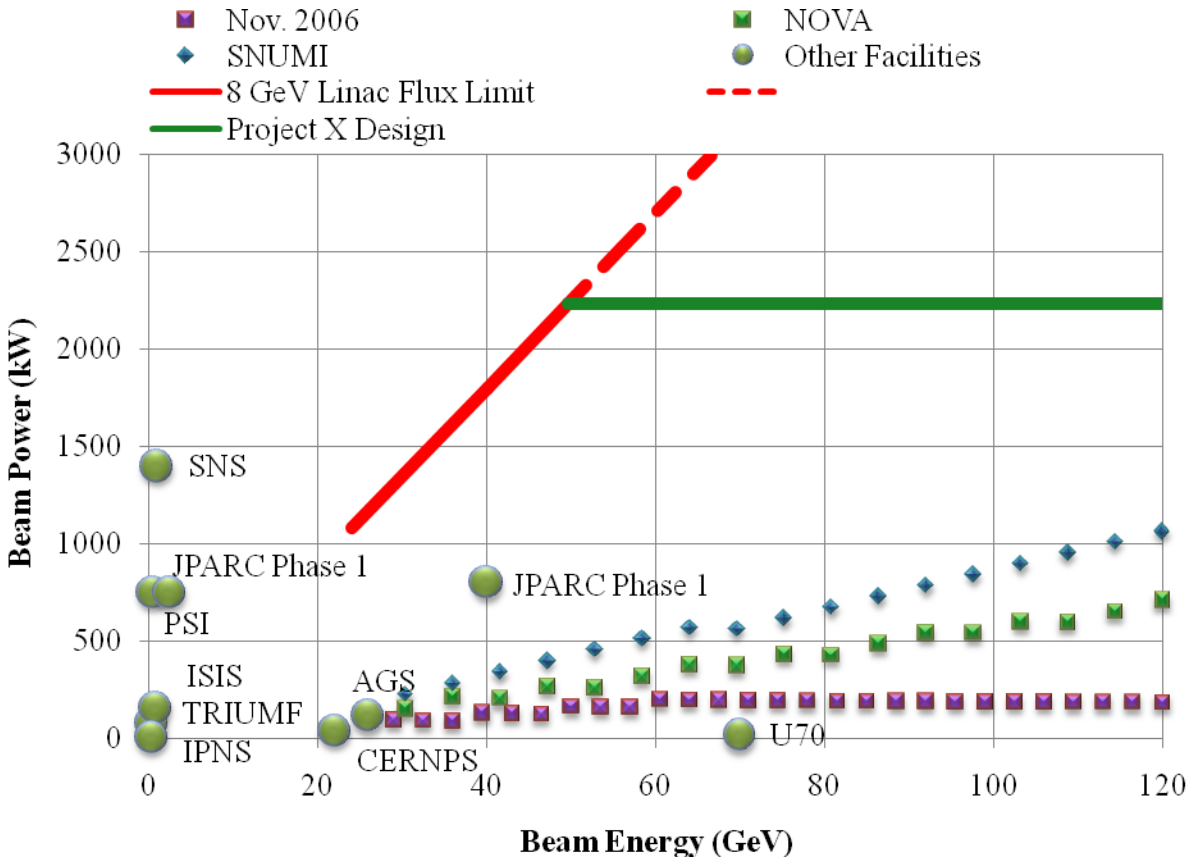

Figure 1.3 Beam power versus beam energy for various proton sources

1.4 Summary

Using the Recycler as a proton accumulator reduces the required charge per pulse in the 8 GeV linac to below the design value of the ILC charge per pulse. With the lower value of linac current, much of the 8 GeV linac can be based on ILC technology. This benefit comes at the expense of space charge and stability issues in the Recycler that arise by storing beam in the Recycler. This document will discuss this issue along with other accelerator physics challenges arising from the concept. This document is not meant to be a design report. The document will discuss the technical issues and possible solutions to the issues. As will be shown later, although there are many challenging technical issues to building an intense protons source as presented in this concept, these issues are surmountable.

This document is divided into six major subsections:

Section 2. The 8 GeV Superconducting Linac

Section 3. 8 GeV H- Injection into the Recycler

Section 4. Proton Accumulation in the Recycler
Section 5. Acceleration in the Main Injector
Section 6. 8 GeV Extraction from the Recycler
Section 7. 120 GeV Beam for Neutrino experiments

Section 2 will explore how similar the 8 GeV superconducting linac can be made to the ILC design. Major issues are transverse focusing and the distribution of accelerating gradient along the linac. The section will present two designs that explore tradeoffs of focusing and accelerating gradient. The section will discuss cryogenic and civil construction issues. This section relies heavily on the comprehensive Proton Driver design report.

Section 3 will review and discuss the issues associated with stripping 8 GeV H- ions. Again much of this work is based on the Proton Driver design report. The section will discuss transport between the linac and the Recycler, techniques for longitudinal and transverse phase space painting, foil issues, injection losses and the injection absorber.

Section 4 will address proton accumulation in the Recycler. It will outline the optimal transverse and longitudinal distributions needed to reduce space charge tune shift to an acceptable level. It will be show that with the addition of a second harmonic in the RF system and phase space painting techniques, the space charge tune shift can be brought down to a level that is comparable to the space charge tune shift at injection in the Main Injector observed during present operations. It will also discuss sources and possible cures of coherent instabilities for high beam currents in the Recycler and Main Injector. In addition, an outline of expected or tolerable beam loss and the radiation resistance of the Recycler's permanent magnets are presented. Also, a sizable section on beam loss management and radiation protection in the Recycler and Main Injector is included.

Section 5 will discuss acceleration of high beam currents in the Main Injector. The parameters for a new RF system and a gamma-t jump system will be presented. The section will also include a discussion of local and non-local beam loss. Much of the discussion of space charge tune-shift, coherent stability, and beam loss management is shared between the Recycler and Main Injector sections.

Section 6 will explore possible options for extracting beam from the Recycler to an 8 GeV physics program. Scenarios for fast and slow extraction from the Recycler are discussed. Fast extraction from the Recycler is straightforward but slow extraction will be difficult. In addition, the technique of transferring beam from the Recycler to the Debuncher ring for slow spill extraction from the Debuncher is summarized.

The last section deals with targeting issues of high power beams extracted from the Main Injector for neutrino production. The section discusses the two possibilities of a new target hall and upgrading the present NUMI target system. There do not seem to be any major problems with building a new target system to handle beam powers of 2MW or greater. The NUMI system would require substantial upgrades to handle powers greater than 2MW. The upgrades use up the redundancies and safety factors of the initial NUMI project. Many of these upgrades are complicated by having to deal with activation of components.

2 The 8-GeV Superconducting Linac

2.1 Overview

The 8-GeV superconducting linac will provide 5.6E13 H- ions in 1 msec pulses at a 5 Hz repetition rate for multi-turn charge exchange injection into the Recycler Ring.

The linac design is based on ILC parameters and designs. It represents a third generation of the 2005 Fermilab Proton Driver Linac design, significantly modified to conform to key ILC parameters and to maximize employment of ILC technical designs and components. Approximately 480 meters of the 670 meter linac would consist of ILC components. This emphasizes the contribution to industrialization of ILC components in the US and minimizes resources otherwise required for alternative designs. The front-end of the linac relies on 325 MHz superconducting RF technology starting at 10 MeV beam energy.

2.2 Linac Parameter Table

Table 2.1 provides the basic operating parameters of the Linac beam and technical systems. The beam current, pulse length, and repetition rate are identical to corresponding ILC parameters. Transverse emittance, energy spread, and bunch length values come from extensive simulations of a reference design that incorporates eight standard ILC RF units. This design and a second, currently-favored concept that has yet to be completely simulated are described in more detail in the next section. Beam parameters of the second design are expected to be comparable to those of the reference design.

Parameter	**Quantity**	**Unit**
Particle Species	H- ion	
Output Beam Energy	8.0	Gev (kinetic)
8-GeV Beam Power	360	kW
Particles per Pulse	5.625	E13
Pulse Repetition Rate	5	Hz
Beam Pulse Length	1	msec
Average Pulse Beam Current	9	ma
Beam Chopping at 2.5 MeV	- 6% at 89 kHz for 700 ns RR/MI abort/extraction gap - 33% at 53 MHz for 'pre-bunching' for transfer to RR	
Particles per Linac bunch	2.73	E8
Nominal Bunch Spacing	3.1	nsec
8-Gev Transverse Emittance	$\varepsilon H = \varepsilon Y = 0.4$	mm-mrad RMS
8-GeV Longitudinal Emittance	2.5E-6	ev-sec/bunch RMS
8-GeV Energy Spread	At Linac output – 2.7 At RR injection – 0.3	MeV RMS
8-GeV Bunch Length	At Linac output – 1.0 At RR injection – 8.6	psec RMS

Table 2.1 Linac Parameters

2.3 Linac Technical Design Description

The front-end of the linac will consist of a 50 keV H- ion source, a commercially fabricated 2.5 MeV RFQ, a Medium Energy Beam Transport including a fast beam chopper, and a 16-cavity room-temperature section to 10 MeV. From this point on, superconducting cavities are employed. Two types of

single spoke resonator structures and one type of triple spoke structure complete the non-ILC section of the linac. This section operates at 325 MHz, exactly ¼ of the ILC frequency. Five 2.5 MW klystrons, similar to those used by JPARC, can provide the required 325 MHz RF power. Transverse beam focusing is provided by superconducting solenoid magnets from the RFQ through the single-spoke sections; superconducting quadrupoles are employed starting in the triple-spoke section. Designs and pre-production of room temperature section components, including the superconducting solenoid magnets, and the single-spoke superconducting cavities are largely completed at this time by the High Intensity Neutrino Source (HINS) R&D program. The charge of the HINS program is to demonstrate performance of such a machine at energies up to 60 MeV.

Table 2.2 and Table 2.3 compare the superconducting sections of the reference linac design to the currently-favored design. The reference design includes eight standard ILC RF units each consisting of 26 cavities and one quadrupole. It employs special "squeezed ILC" cavities and cryomodules to cover the non-relativistic β=0.8 energy region. The "squeezed ILC" section is eliminated in the second design, replaced by four additional triple-spoke cryostats and two ILC RF units with the $8\pi/9$ mode of the ILC cavities tuned to the accelerating frequency. Eleven additional ILC RF units complete the linac. Transverse optics considerations require that the six $8\pi/9$-mode cryomodules and nine "ILC-1" cryomodules each contain two quadrupoles with seven ILC cavities. The "ILC-2" section consists solely of cryomodules of the standard ILC 'eight cavity - one quad' design type. The final four RF units, 28 cryomodules, are the standard ILC 9-8-9 cavity configuration.

PROTON DRIVER Ending w/8 ILC RF Units								
Section	SSR-1	SSR-2	TSR	S-ILC	ILC 8pi/9	ILC-1	ILC-2	ILC
End Coordinate	31.4	61	142	227	227	336	336	640
Beta Design	0.2	0.4	0.6	0.8	n/a	1	n/a	1
Output Energy (MeV)	30	120	420	1200	1200	2800	2800	8000
# Cryomodules	2	3	7	7	n/a	9	n/a	24
# Cavities/cryomodule	9	11	6	8	n/a	7	n/a	9-8-9
# quads/cryomodule	9	6	6	4	n/a	2	n/a	0-1-0
Slots"/cryomodule	18	17	12	12	n/a	9	n/a	9
# Cavities (total)	18	33	42	56	n/a	63	n/a	n/a
Max Nom. Accel. Gradient	10	10	10	25	n/a	31.5	n/a	18.3/31.5
# RF Units	325 MHz	325 MHz	325 MHz	2.33	n/a	3	n/a	8

Table 2.2 Superconducting sections of reference linac design with 8 ILC RF Units

PROTON DRIVER w/ 8pi/9 ILC Section								
Section	SSR-1	SSR-2	TSR	S-ILC	ILC-8pi/9	ILC-1	ILC-2	ILC
End Coordinate	31.4	61	188	188	262	373	521	669
Beta Design	0.2	0.4	0.6	n/a	1	1	1	1
Output Energy (MeV)	30	120	603	603	1040	2390	5150	8000
# Cryomodules	2	3	11	0	6	9	12	12
# Cavities/cryomodule	9	11	6	n/a	7	7	8	9-8-9
# quads/cryomodule	9	6	6	n/a	2	2	1	0-1-0
Slots"/cryomodule	18	17	12	n/a	9	9	9	9
# Cavities (total)	18	33	66	n/a	42	63	96	104
Max Nom. Accel. Gradient	10	10	10	n/a	31.5	31.5	31.5	31.5
# RF Units	325 MHz	325 MHz	325 MHz	n/a	2	3	4	4

Table 2.3 Superconducting sections of the favored linac design including $8\pi/9$ mode section

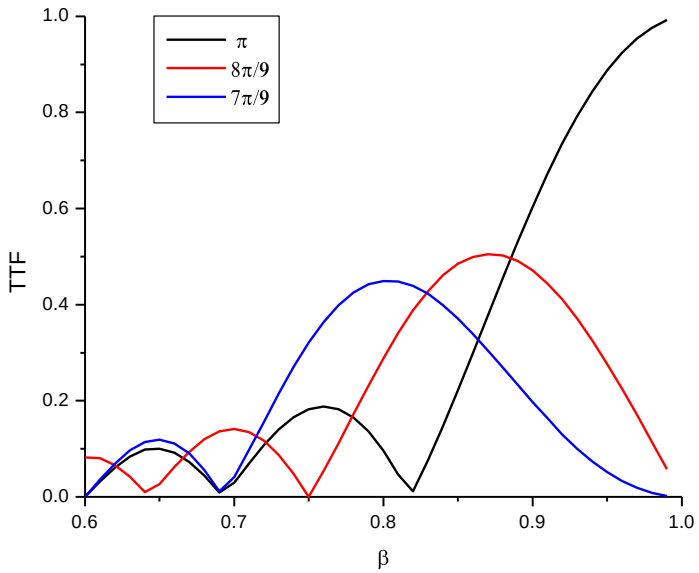

Figure 2.1 Transit time factors of cavity modes versus particle velocity

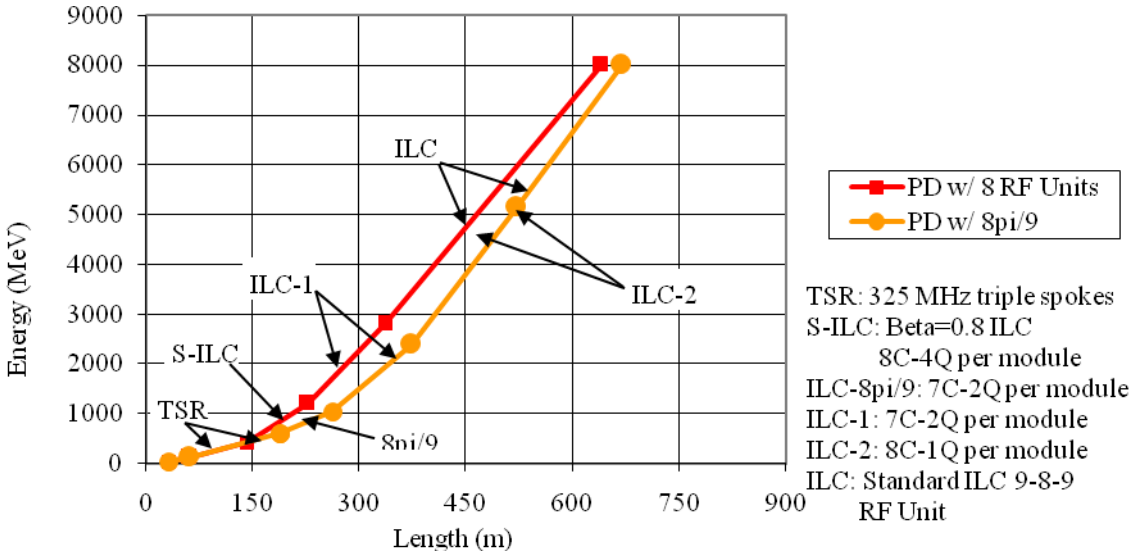

Figure 2.2 Endpoint Energy vs. length for two linac designs

The motivation to exploit the 8π/9 cavity mode is to maximize the number of ILC beamline components. As shown in Figure 2.1, this mode offers the opportunity to recoup acceleration efficiency that diminishes rapidly for the normal ILC cavity π-mode in the β=0.9 energy range due to the transit time factor.

Figure 2.2 shows that the length of the two designs is quite similar. Inefficiencies of the 8π/9 section relative to the "squeezed ILC" section are compensated by operating all final eight RF units at 31.5 MV/m. In the reference design, four of those units are run at 18.3 MV/m to control RF defocusing at low energies given the sparse quadrupole distribution.

With either design, one additional ILC klystron RF system is required in the transfer line downstream of the linac to power four 17-cell copper debuncher cavities to reduce momentum spread of

the beam entering the Recycler. The debuncher system is not superconducting due to its remote location with respect to any cryogenics infrastructure.

Longitudinal dynamics of the non-relativistic H- beam require active control of RF amplitude and phase on a cavity-by-cavity basis although many cavities are to be powered by a single klystron. This is accomplished by including high power fast ferrite vector modulators in the RF distribution system throughout the linac with the exception of the final four ILC 9-8-9 RF units. All cavities, fast modulators or not, require that the static phasing of the RF distribution system be set as required by the H- beam.

The machine design will include the possibility of electron beam acceleration through eleven ILC RF units (~8 GeV) with suitable re-adjustment of cavity phasing and quadrupole currents. It is to be a manual operation to switch between electrons and H-; pulse-to-pulse switching is not supported in this design.

2.4 Physics and Technical Issues

2.4.1 Physics Issues

The HINS R&D program as presently defined will resolve some major physics issues of the 8-GeV linac. This program is intended to demonstrate:

- Beam acceleration in spoke loaded SC cavities
- H- beam acceleration in multiple cavities fed by single klystron
- Phase and amplitude control of cavity fields by high-power fast ferrite vector modulators
- Beam chopping at 53 MHz repetition frequency
- High beam quality in the linac with solenoid focusing
- Negligible effect of HOMs on beam quality in a proton/H- linac

Additional major physics issues that would remain to be resolved include:

- Demonstration of phase-locked operation of 9-cell ILC cavity on the $8\pi/9$ mode.
- Transient beam dynamics analysis in the linac with realistic RF distribution and feedback system.
- Definition of any potential project upgrades that are not to be excluded by the design of the 8-GeV linac.

2.4.2 Cryogenics Considerations

Cryogenic system operating temperatures and pressure levels for the 8-Gev linac are largely determined by the choice of the ILC style cryomodules and the design of the 325 MHz front end linac. The ILC cavity cold mass structure operates at 2 K temperature. The 325 MHz front end linac is cooled by 2-phase helium at 4.5K.

The scope of the 8-GeV linac cryogenic system includes cryogen production and distribution. A helium refrigeration plant similar in scale to that at the Spallation Neutron Source at ORNL will be required. System components include the cryogenic plant, compressors, cooling towers, auxiliary systems, distribution and interface boxes, non-magnetic and non-RF cold tunnel components, and cryogenic transfer lines.

The feasibility of early commissioning using LN2 in the shields of the ILC-style cryomodules should be investigated. This could prove attractive for the schedule if the Fermilab CHL can be used for early, albeit cryogenically inefficient, commissioning of the Linac. Nevertheless, a completely new plant is anticipated within the scope of the project.

Most major components of the 8-GeV cryogenic system have been used successfully in similar systems before. Nevertheless, the 8-GeV linac cryogenic distribution system presents challenges including:

- Liquid level control in long strings of helium vessels filled by means of series flow under conditions of large dynamic heat loads from RF power and very long time constants. A

conceptual design for electric heaters, to counteract the impact of sudden heat load changes, needs to be developed and the impact on total heat load evaluated. The flow pattern and cooling limitations of two-phase superfluid helium must be studied and validated with respect to slope and string length.

- Heat load estimates of the ILC cryomodules as well as uncertainty and overcapacity factors all need refinement.
- Optimization studies for capital and operating costs needs to consider tradeoffs of cryomodule complexity vs. heat loads.
- Protection from over pressurization due to abnormal operating conditions, such as loss of beam tube or insulating vacuum, power outage, etc., must be designed. Vacuum isolation, lengths of vacuum units, and fast-acting vacuum valves all need further investigation. The 2 K cavity-cooling circuit is most critical due to the low pressure limits imposed by the niobium RF cavities, but the thermal shield flow circuits may also be difficult to protect.
- Compliance with engineering standards and the associated component design pressures must be studied with respect to cost, operability and reliability.

These are all cryogenic system issues that ILC must also address.

2.4.3 Civil Site Considerations

As described at the 8-GeV Linac Director's Review in 2005, the site for an 8-GeV linac injecting into either the Main Injector or the Recycler is subject to numerous rigid constraints. These include limited straight sections in either machine lattice adaptable to the injection system, site boundary considerations, existing facilities, retaining nearby space for future possible experiments or facilities (e.g. a proton accumulator ring for possible future muon production), and accommodation for the large bending radius necessary for any 8-GeV H- transport line to prevent magnetic field stripping. There is no new evidence to suggest a more suitable site for an 8-GeV linac at Fermilab than inside the south half of the Tevatron ring.

The entire southern half of the area inside the Tevatron Ring has been professionally characterized for environmental considerations as well as for soil and earth constructability. There will be a wetlands impact, for example, but all possible sites in that general area meeting the various criteria outlined above are similar. The Army Corps of Engineers was consulted and it is likely that either the purchase of off-site offset credits, or the construction of off-site mitigation, will be the preferred mitigation option, so the on site location of this proposed project may be set without reference to particular narrow considerations. The total mitigated off-site area will probably be on the order of 120 to 160 acres for the project now under consideration.

3 8 GeV H- Injection into the Recycler

3.1 Introduction

The objective of a stripping injection process is to overlay an incoming H^- beam from the linac on a circulating H^+ (proton) beam in the ring. The stripping of two electrons is accomplished by a thin stripping foil (Figure 3.1). This is a non-Liouvillean process allowing for a great flexibility in phase-space painting with an improved beam distribution and, thus, for minimized space-charge effects. However, the circulating protons are allowed to pass through the foil several times, thus creating beam losses and heating the foil.

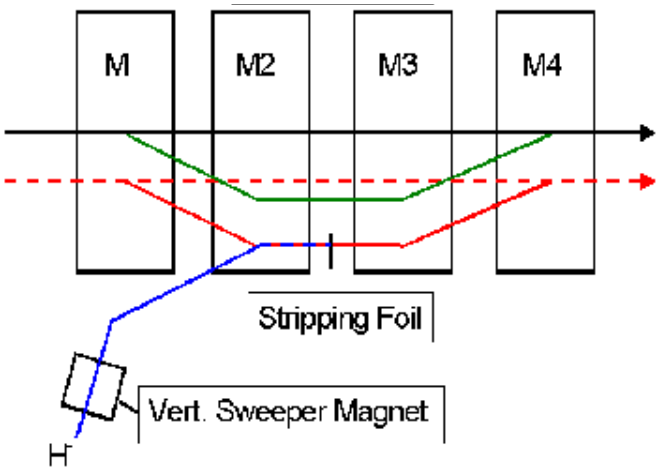

Figure 3.1 Schematic of a stripping foil injection. Closed orbit bump magnets move circulating particles out to combine with incoming H^- beam. The vertical sweeper magnet is used to create a particular transverse phase-space distribution. The closed orbit is moved back at the end of the injection.

Increased foil thickness improves conversion efficiency of H^- to H^+ but at expense of increased beam Coulomb scattering and nuclear interactions. Balance suggests thickness of ~500 μg/cm^{-2} is appropriate and will convert ~99% of H- beam to protons. Additional drawbacks for using a foil is a relatively short foil lifetime and activation of foil support beamline component.

As an upgrade option, we considered laser-based stripping, with a scheme similar to what is being developed at SNS. This option will require more design studies and goes beyond the scope of this paper.

3.2 Previous Experience with H- multi-turn injection

The Linac produces H- ions with a kinetic energy an order of magnitude higher than the 800 MeV H- beams routinely handled at LANL, and a factor of six higher than the SNS 1.3 GeV upgrade. To verify that no problems were foreseen with H- transport and injection at these energies, a workshop[2] with experts in the field was held in December 2004. H- transport issues addressed included H- stripping from magnetic fields, beam line vacuum, blackbody radiation, and other possible sources of beam loss. The workshop also discussed H- injection issues, injection foil issues, and transport line collimation issues. One new effect, the stripping of H-

ions by room-temperature blackbody radiation, was identified. The conclusion[3] of the workshop was that the design parameters of the Proton Driver [4] transport line were valid and the performance could be reliably extrapolated from current experience.

Subsequent to the workshop, a Director's Preliminary Technical review of the Proton Driver was held in March 2005.[5] Many of the issues raised in this review have been addressed which has resulted in a revised transport line design and revised Main Injector straight section and injection system design. In addition, an MOU with BNL is in place to aid in the optimization of the foil-stripping injection system and work is on-going.

Although the previous work was performed with the Main Injector as the injection accelerator, a provision was included in the beamline for a vertical achromat to transport the beam to the Recycler elevation for injection. The description here is based upon the previous body of work with extensions or extrapolations to the ILC Linac beam parameters and pulse length and repetition rate.

3.3 H- Transport from Linac to Recycler

Transport from the end of the linac to the injection point of the Recycler will be accomplished by a low loss transport line capable of providing betatron and momentum collimation, phase rotation for energy spread reduction, diagnostics for beam characterization, and flexible matching into the Recycler. As part of the previous Proton Driver study, a transport line has been designed which incorporates these functions. [6] The current lattice and dispersion for the MI injection beamline is shown in Figure 3.2.

The first section (A) after the linac is a betatron matching straight section where the four gradients are adjusted to match the beam from the linac into the 60 degree FODO straight section. This section is flexible and has been used to match lattice functions from the PD and the ILC linac beam parameters.

Halo collimation is contained in the first section after the matching section, section B. The phase advance in the transport line is 60 degrees, so three pairs of horizontal and vertical collimators are used. Each pair consist of a thin stripping foil located upstream of a quadrupole and absorber located at the end of the downstream straight section. Both foil and absorber are movable apertures. The foil strips large amplitude particles which are separated by the downstream quad to produce an offset at the downstream absorber, a technique utilized by SNS.[7] It is envisioned that this collimation system will be used to shape the beam profile on the foil and minimize H- missing the foil.

The main body of the transport line consists of two reverse bend achromats (C &E) separated by a straight section (D). The dipole field and straight section length are determined by minimizing Lorentz stripping and siteing considerations and well as providing enough drift for a phase rotator cavity in the injection matching section.

The injection matching section was designed to accommodate a vertical switch in a similar fashion to the vertical switch to be used in the Nova project to transport 8 GeV protons from the 8 GeV line into the Recycler. Although preliminary calculations have been made and dipoles included in lattice files for the Proton Driver solution, detailed design of the vertical achromat incorporated within the matching section needs to be done.

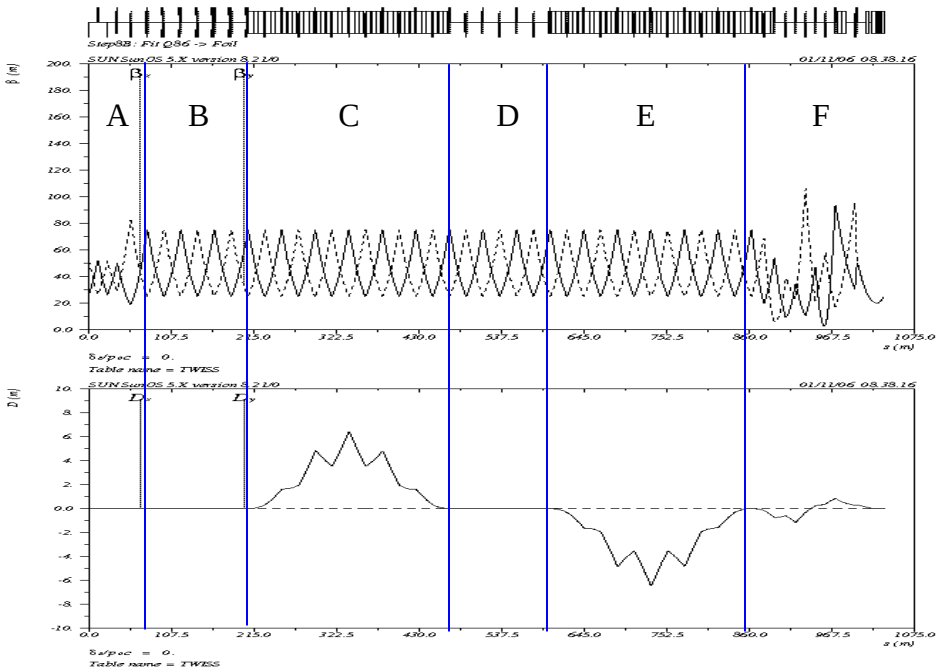

Figure 3.2 Lattice function and dispersion of the linac to MI transport line designed for the Proton Driver project. The sections are: A) matching, B) betatron (halo) collimation, C) CW achromat with momentum collimation, D) straight section, E) CCW achromat, and F) injection matching achromat with longitudinal phase rotator.

Loss control at high beam power is critical for hands on maintenance. Local residual activation levels of 100 mrem/hr at one foot is considered at the limit under ALARA. Average residual levels should be on the order of 20 mrem/hr or less. On an unshielded beam pipe, 100 mrem/hr corresponds to 0.25 W/m. which implies that the average loss through the beamline should be considered at or below 0.05 W/m. See section 4.3.2 for further discussion.

Two general classes of beam loss are generally considered in transport line/accelerator design. The first is due to the beam hitting an accelerator (or transport line) structure either on purpose (controlled) or by accident (uncontrolled). This can be minimized by making the ratio aperture/beam size as large as economically possible. The dipole magnets in the transfer line will be recycled B2 magnets with a 4" by 2" horizontal and vertical aperture. The majority of the quads may either have a 3" round or star shaped chamber. Larger quad apertures will be required is selected quads of the matching section due to the larger amplitude functions at the end of the linac. The ratios are summarized in the Table 3.1 with the minimum ratio in the current Proton Driver transfer line design of 3.5 in the vertical dimension with a cryo-beam liner.

	Horizontal (D=0)	Horizontal (D=6.4)	Vertical
Quad (round)	6.8	3.3	5.8
Quad (star)	10.5	5.1	5.7
Dipole(w/liner)	8.7	4.2	3.5

Table 3.1 Ratio of Aperture to Beam Size in different beam pipes.

The second class of beam loss is due to single particle mechanisms such as beam particles interacting with residual gas, Lorentz stripping of the weakly bound second electron, and photo-detachment due to present black body radiation in the beam pipe.

Preliminary estimates of gas stripping loss rate have been reported[8] assuming same vacuum level as the current A150 line with similar components, as 10^{-7}/m. The lab frame lifetime and loss rate have been calculated as 8.7 sec. and 3.8×10^{-10} /m for a field of 500 Gauss. The dipole magnetic field has been selected as ~480 G based upon stripping considerations and site selection considerations. The beamline will have new quadrupoles with 3 inch pole tips and gradients of ~10 kG/m which give pole tip fields of 375 Gauss. At this pole tip field no significant Lorentz stripping takes place within the quad

The most significant source of beam loss is due to the black-body photons, present in a vacuum chamber which is Doppler-shifted to a sufficient energy to strip the weakly bound electron (0.75 eV) from an H- ion. The black body radiation loss rate at room temperature (300K) has been estimated to be 8×10^{-7}/m.[9] This would generate an average residual activation level of > 100 mrem/hr on exposed beam pipe and ~20 mrem/hr on magnets. A reduction of the temperature of the internal surface of the vacuum chamber wall will reduce the overlap between the black-body spectrum with the H- photo-detachment cross section, thus reducing the loss rate. A preliminary design has been done for an extruded Al extruded beam pipe liner with super insulation shield to be operated at LN2 or GN2 temperatures.[10] A internal heat load of 1 W/m and external load of 3 W/m were assumed. This is similar to work done for cryo piping for SSC and LHC cryostats. It was shown that with flow only in one corner, that the temperature can easily be maintained. One would anticipate building these into the initial design to reduce beam loss due to black body radiation. The impact on the detachment rate due to black-body radiation at 77oK is to reduce the rate by about 3 orders of magnitude. This would also reduce the gas stripping on loss rate, although the magnitude of the reduction has not been calculated to date.

If the initial linac current is 9 mA with a 1 ms pulse length (with no chopping) and a 5 Hz rate , this corresponds to an average beam power of 360 kW assuming all 325 MHz bunches have beam. For the neutrino program, only three of the linac pulses are required which brings the beam power to 154 kW for the neutrino program. In reality, some of the bunches will be chopped at 2.5 MeV for matching the 53 MHz bunch structure in the Recycler and to create a beam abort gap in the Recycler. The linac still has 4/7 the power, or 206 kW for other 8 GeV programs. All the calculations for transport and injection will assume all beam bunches are filled. Table 3.2 summarizes beam loss rates and power associated with the three identified processes for the initial beam power with and without the beam screen and an ultimate intensity with the shield. It should also be pointed out that the beam loss for black body and Lorentz stripping is not uniform throughout the transport line and detailed loss simulations should be carried out. The tracking program STURCT has this capability and the above loss mechanisms are being implemented into the program TRACK. End-to-end simulations, from the RFQ to the injection foil have been completed using TRACK and the addition of these stripping mechanisms will provide a more complete picture of the transport and loss distribution for 8 GeV H- acceleration and transport to the injection foil.[11]

3.4 Injection Straight Section Optics

As a result of the Directors Review the Main Injector MI-10 straight section was re-design to allow for H- injection.[12] The modification involved changing the straight section from a FODO lattice (with 17.28m half-cell) to a symmetric straight section with 38 meters of drift

between quad doublets. This drift length provides the required space for the injection chicane and injection absorber transport line, decouples the tuning of the injection system from the ring tune (no quads within the injection system), provides a flexible lattice with the foil located at a beam waist, allows for only a drift to be between the foil and absorber with the optics being determined by the transport line matching into $\alpha_x \sim \alpha_y \sim 0$ (i.e. a long waist). Figure 3.3 shows the re-designed straight section. Figure 3.4 shows the beam envelope at the foil and absorber.

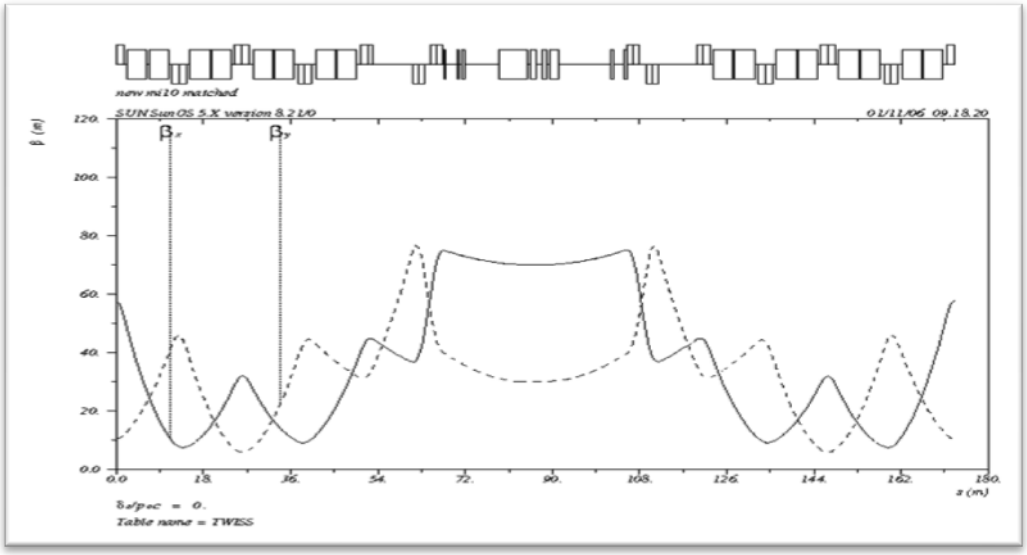

Figure 3.3 Symmetric straight section created for the Main Injector for H- injection.

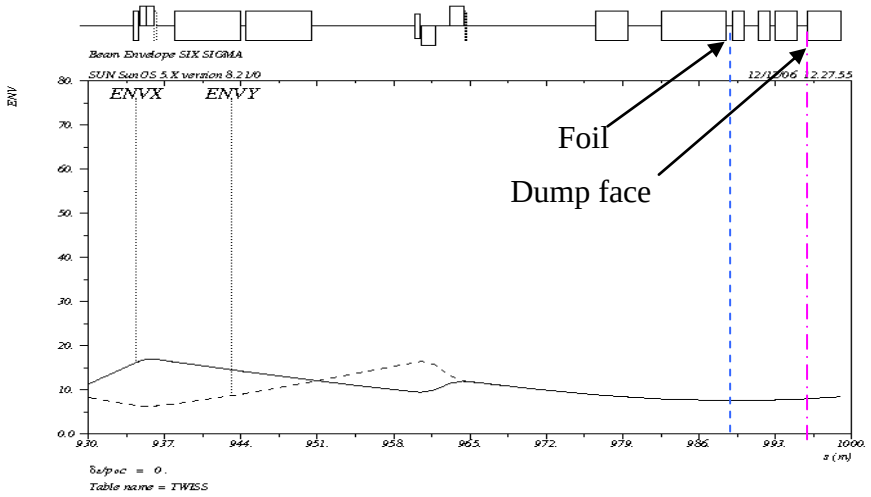

Figure 3.4 Six sigma beam envelope through the end of the injection line for an emittance of 4.5 π-mm-mr H- from the linac.

The current Recycler lattice was patterned after the MI lattice but with permanent magnet gradient magnets and quads and a phase trombone at the 60 straight section. The Recycle 10 straight section optics is that of a 90 degree FODO lattice. The current expectation is that the Recycler injection straight will be patterned after the MI. This modification will require a

combination of new permanent magnet gradient magnets and quads and the addition of electromagnet quad trims.

	360 kW		360 kW with shield		2.1 MW with shield	
loss mechanism	[m^{-1}]	[w/m]	[m^{-1}]	[w/m]	[m^{-1}]	[w/m]
Black body	8.00E-07	2.88E-01	8.00E-10	2.88E-04	8.00E-10	1.73E-03
Residual Gas (A150 10^{-8} torr)	1.00E-07	3.60E-02	1.00E-10	3.60E-05	1.00E-10	2.16E-04
Magnetic (500 G)	3.80E-10	1.37E-04	3.80E-10	1.37E-04	3.80E-10	8.21E-04
Total	9.00E-07	3.24E-01	1.28E-09	4.61E-04	1.28E-09	2.76E-03

Table 3.2 Summary of loss rates for initial and ultimate linac power assuming all pulses have beam

3.5 Transverse Painting

The transverse distribution required for Recycler injection to minimize space charge tune shift is that of a KV-like uniform distribution. The required normalized emittance is 25 π-mm-mr in both planes. The desired KV distribution is described by the following distribution function in particle action variable, *I*:

$$f(I) = \frac{1}{I_{\max}} \times \begin{cases} I, \ I \le I_{\max} \\ 0, \text{otherwise} \end{cases}$$

where *I* represents the normalized action variable in either *x* or *y* planes, such that for a given particle $I_x+I_y=const$ and I_{max} = 25 π-mm-mr. Such a distribution requires anti-correlated phase-space painting in two transverse planes. Transverse phase space painting algorithms were proposed by KEK and have been incorporated in to the program STRUCT[13] and utilize a horizontal orbit bump, which paints from the inside of the accelerator phase space to the outside of the phase space. This means that the painting bump had a maximum displacement on turn 1 with a magnitude of σ_{x11} which collapsed to zero at the end of painting, moving the circulating beam off the foil. The resulting maximum horizontal beam size at the foil location is $(I_{max}\beta_x/\beta\gamma)^{1/2}$ = 13.5 mm. The vertical painting is generated by ramping the input vertical angle at the foil from ϑ_{MAX} to zero, while keeping the vertical position constant on the foil.

Multi-turn injection painting schemes for the Proton Driver assumed either a 3 ms (270 turn) or a 1 ms (90 turn) injection for a constant load of 1.54E14 protons. Since the pulse length of the ILC Linac is 1 ms with a repetition rate of 5 Hz and a 9 mA beam current, it requires three linac pulses to fill the Recycler with 1.5E14 protons. Figure 3.5 shows a cartoon of painting the full phase space in three injections and removing the phase space from the foil. The arrows represent movement of the central trajectory during the three injections. The painting waveform can be modified such that the three 1 ms linac cycles would be equivalent to the painting waveform used for the 3 ms injection into the Main Injector.

To minimize circulating beam interaction with the foil, the closed orbit must be moved from the foil during the 20 K turns between of each 1 ms linac beam cycles. This may be accomplished by the same type of power supply developed for the fast ferrite phase shifters under the HINS R&D project.[14] The power supply could have a rise/fall time on the order of 100 us (10 turns) and duration of 200 ms. This concept is shown incorporated in the 3 ms painting waveform in Figure 3.6. Here the time scale of the 20K turns is reduced by a factor of 1000 to illustrate the painting waveforms. So, it is essentially three 90 turn injection periods with the closed orbit moving << 1 sigma off the foil each injection.

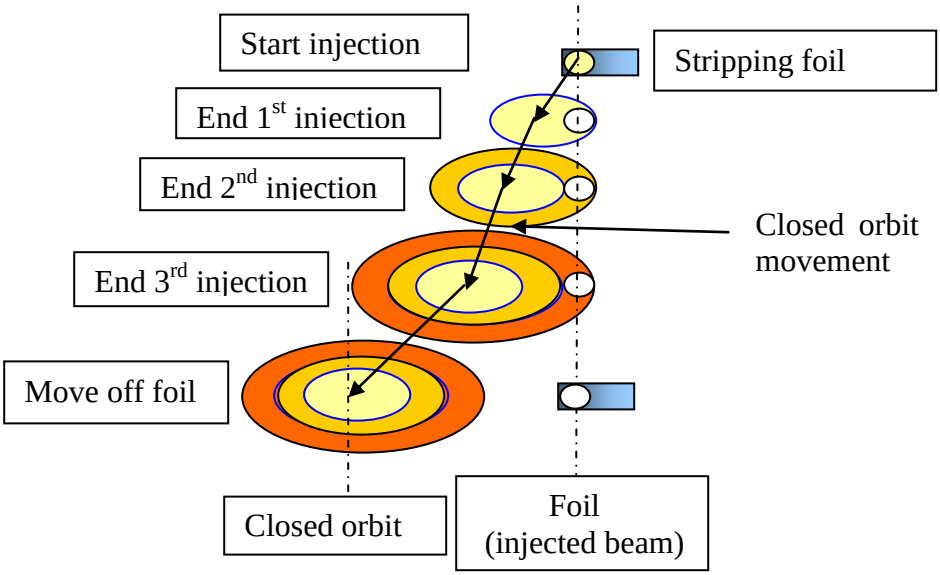

Figure 3.5 Cartoon of horizontal transverse phase space painting showing the relationship between the injection foil, H- beam, the injection orbit, and the closed orbit. It shows how the phase space is built up. NOTE: Any motion between injections is not illustrated.

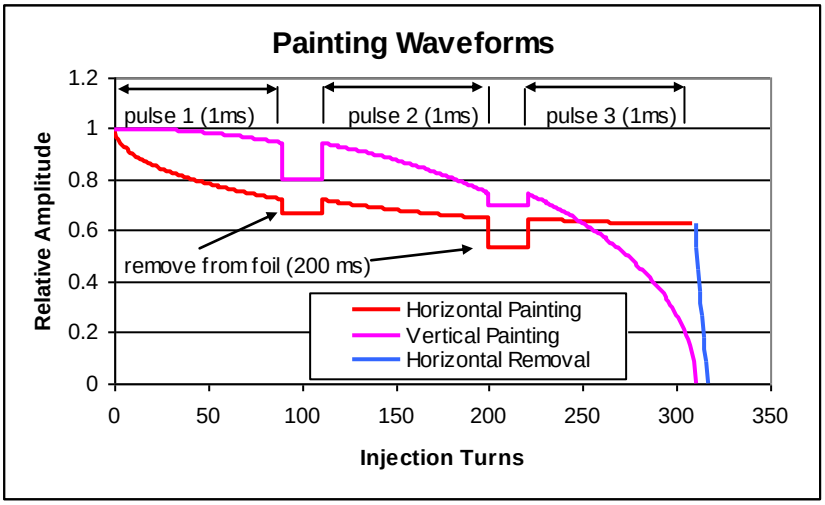

Figure 3.6 Painting waveform for horizontal and vertical transverse painting. The waveform was modified from the 3 ms (270 turn) injection to add in the two notches which represent the time between injections. The horizontal scale has not been modified to show 20 K turns, but rather shows 20 turns for each removal.

3.6 Foil Issues

Utilization of thin carbon foils for stripping electrons from H- ions have been used for many years. Theoretical predictions have been compared with measurements for energies up to 800 MeV. Extensions to the theory have been described and stripping efficiencies and excited state fractions have been calculated for 8 GeV H- incident on thin carbon foils which are consistent with measured excited state fractions at lower energies. The foil thickness that was under consideration for use in the Main Injector injection system was on the order of 400 to 500 $\mu g/cm^2$. The specific thickness used in transverse painting and foil temperature calculations was

425 $\mu g/cm^2$, which has a thickness of 2.1 microns, for Proton Driver intensities into the Main Injector. Table 3.3 lists the charge state fractions for two carbon foils in the above thickness range.

Charge State	425 $\mu g/cm^2$	525 $\mu g/cm^2$
H+	97.6	99.1
n=1	1.68	0.59
n=2	0.56	0.20
n=3	0.15	0.056
H-	.0022	1.6E-4
Total H+ captured	97.75	99.17

Table 3.3 Charge state fractions (in percent) produced in various carbon foil thickness

The location of the stripping foil and the magnetic design of the magnetic chicane elements are such that n=1 and 2 fractions are not stripped in the downstream magnetic field and these are converted to protons at a secondary stripping foil and sent to the injection absorber located immediately downstream. The capture of the n=3 states are dependent on the end-field shape of the downstream chicane magnet. It will be necessary to utilize a flux catcher to clamp the end field and reduce the spread in stripping angles produced by the lifetime of the n=3 excited states. All states higher than 3 strip immediately and are captured in the circulating beam emittance. Any H- that misses the foil and any H- that is not stripped in the foil will be field stripped (converted to H0) over a short range in the end field of the downstream chicane magnet and subsequently be stripped to protons by the secondary foil. The differential angles of the H0 due to Lorentz stripping in the end field of the chicane magnet are less than 0.5 mr which would imply less than 1 mm position spread at the secondary foil and less than 5 mm spread in position at the injection absorber, easily contained within the vacuum chamber.

The foil dimensions and orientation play an important role in determining if any beam halo miss the stripping foil and the number of secondary hits on the foil. The SNS injection system had some issues with the trajectories of the H- halo missing the foil and the H0 excited states not being cleanly transported to the injection absorber. To remedy this situation the optics in the injection absorber line were modified and the transverse size of the injection foil was increased thus increasing secondary foil hits by the circulating beam.[15] To circumvent these issues, several design choices for the Main Injector injection system were chosen. First, the halo produced by the linac is cleaned up by a betatron collimation system located at the upstream end of the transfer line. This will be used to shape the beam profile on the stripping foil which will minimize the amount of halo missing the foil. The foil active area and position will be sized such that it corresponds to the predicted spot size plus a tolerance for steering. The beam spot size is adjustable dependent on the linac emittance.

Foil heating and maximum temperature simulations have been done for Proton Driver beam intensities (1.5E14/pulse) and repetition rates of 10 Hz and 1.5 sec.[16] The peak temperature is a linear function of intensity and strong function of initial spot size and to a lesser extent the injection pulse length. Secondary hits on the foil are more or less uniformly distributed and do not impact the peak temperature to a significant extent. For initial H- beam sigma of 1 mm the peak temperature reached upwards of 2200 ^oK. Since the ILC linac pulse intensity is a factor of 3 lower the peak temperature is expected to be down by a factor of 3 to a level of 700-750 ^oK . Foil lifetime tests have shown that lifetimes fall dramatically above foil temperatures of ~1700^oK

Peak foil temperatures are expected to be a factor of 2 or more lower than this value for Project X intensities. The simulation contains heat radiation from the foil. After the initial energy transfer from the 1ms beam pulse, heat radiation reduces the foil temperature till the next pulse arrives. If there is sufficient time, the foil temperature approaches ambient temperature. The equilibrium temperature, for a given configuration is a function of the peak temperature and repetition rate. For the longer repetition rate the foil cooled back down to ambient temperature while for the 10 Hz case the foil reached an equilibrium temperature of roughly 600 ^{o}K . For the 5 Hz case with the lower instantaneous intensity (temperature) the peak and equilibrium temperature are expected to range between ambient and 700 ^{o}K if the beam sigma is at the 1mm level. For larger spot size the peak temperature will be reduced on the order of 68% for an increase in sigma to 1.5 mm. None of these temperatures are expected to be an issue with foil survivability. New diamond carbon foils[17] have been produced which are more rigid (for easy support)and heat tolerant. Utilization of these foils in a stripping system is expected to produce a robust foil system.

The foil is to be located on the median plane in the rising end field of a 0.55 T chicane magnet at a field strength of approximately 600 G with the magnetic field perpendicular to the trajectory. The electrons will see an increasing field magnitude as they travel from the foil. Simulations using an expected end field shape show the electrons have an average bending radius of about 5.5 cm where they can be collected downstream of the foil on an external electron catcher.[16]

The nuclear collision length for carbon is 60 g/cm2. For a foil thickness of 500 μg/cm^2 the probability of a nuclear collision is ~ 8E-6. The resultant shower will impact the activation of downstream elements dependent on the geometry and number of total collisions. The activation of particular elements and expected residual activation levels should be simulated with a code such as MARS. For an intensity of 2E14/sec and 4 secondary foil hits per circulating proton one would expect ~6E9 interactions/sec.

While the proton beam emittance growth due to multiple coulomb scattering on the foil is negligible, the single large-angle Coulomb scattering leads to injection losses and halo formation, as described below in section “Injection losses”.

3.7 Longitudinal Painting

The Recycler longitudinal emittance at injection must be matched to that of the Main Injector. The specified longitudinal emittance of the Main Injector that satisfies constraints due to longitudinal instabilities and transition crossing is 0.5 eV-sec. A dual harmonic RF system is envisioned to produce a more uniform longitudinal bunch distribution. The ratio between first harmonic and second harmonic voltage has been found to be one-half for the second harmonic. The requested 1st harmonic voltage has been specified to be 750 kV giving a bucket area or 0.8 eV-sec and a 99% bunch emittance of 0.5 eV-sec.

Longitudinal simulations[16] have been performed for microbunch injection into the Main Injector for 1st harmonic RF voltage of 400 kV. The maximum dE that was allowed was +/- 15 MeV. The bucket area was 0.56 eV and the rms bunch emittance was 0.047 eV-sec. Longitudinal space charge and longitudinal painting due to only phase slippage between the 325 Mhz and MI frequency were included in the simulations. The broad band impedance has not been included. If longitudinal painting in energy is required, this can be easily accomplished by ramping the central phase of the debuncher cavity at the end of the transfer line. Additional simulations are planned to include the new bunch requirements and investigate painting in energy.

3.8 Injection Losses

With 360 kW of injected beam current, it becomes critical to keep beam loss under control. One must address the losses in the immediate injection area due to the first turn interaction of the H- with the injection system (magnetic field, residual gas, foil interactions and misses) as well as the interaction of the circulating protons with the stripping foil which could give rise to immediate loss and/or the formation of beam halo. At present, the measured horizontal admittance, A_x of the Recycler, configured as a pbar storage ring, has been measured as ~66 π-mm-mrad and the vertical admittance is a factor of two smaller.[18] It is possible to increase the vertical admittance to above 40 π-mm-mrad by removing several pbar-specific elements. At the writing of this report, we decided to limit both admittances to 40 π-mm-mrad, assuming that the adequate collimation system will be designed and installed in the Recycler.

The following processes and their contributions have been identified. Estimates on the magnitude of th loss are given but a detailed simulation of activation levels, using a code such as MARS, due to these losses needs to be done.

- First turn H- missing foil: less than two percent of the incident beam. This can be minimized by beam shaping using betatron halo collimation at the entrance to the transfer line.
- First turn H0 excitated states stripping and falling outside the acceptance of the ring. This will be minimized by specifying the peak field of the chicane dipole to be less than the n=1 and 2 H0 principle states (between 1 and 2%) and tayloring the end field fall off to minimize the range of angles where the n = 3 excited states (less than 0.2%) strip.
- Multiple scattering in foil: This is minimized by making the foil as thin as possible. Only large amplitude particles interacting with the foil would contribute to halo.
- Energy straggeling in foil: This would contribute to longitudinal emittance dilution. Preliminary estimates show for the foil thickness in discussion the maximum energy loss is less than 80 keV.
- Nuclear interaction with foil producing hadronic shower: This rate has been estimated as 6E9 particles/sec. This needs to be simulated. This is reduced only be reducing the number of foil hits and reduction in foil thickness.
- Electrons from stripped by foil: These are to be "caught" be an electron catcher outside the beam pipe designed to minimize the production of secondary electrons. This device has yet to be designed.
- Circulating protons interacting with foil undergoing nuclear collision: This will be minimized by minimizing the foil size within constraints on incoming beam size and foil temperature and the details of the painting function.
- Single large-angle Coulomb scattering create beam halo. Figure 3.7 presents the transverse beam distribution after a single passage through a 500-μg/cm^2 foil for an ideal KV beam with I_{max} = 25 π-mm-mrad. From this figure one can see that the relative number of particles scattered outside of the 40 π-mm-mrad admittance is about 7×10^{-5}. Assuming there are a total of 5 foil passages, this number will be about 4×10^{-4}. This means that the Recycler injection collimation system should be able to handle at least 150 W in each plane for this effect alone.

3.9 Injection Absorber

The injection absorber is required to collect unstripped H- and H0 from the injection foil. A compact injection absorber design has been discussed[19] for the Proton Driver which would

handle a nominal 5% of 132 kW (8 GeV injected power of the Proton Driver) and yearly intensity of 1E20 protons/year. The prompt radiation in the MI10crossover, soil activation and residual activation are well within acceptable limits. In addition the temperature in the core is well within cooling limits. Extrapolating to to Project X injection intensities, a 5% loss of 360 kW into the absorber would require 18 kW capability, a factor ~3 over initial design criteria. Additional shielding calculations are required for the increased intensity.

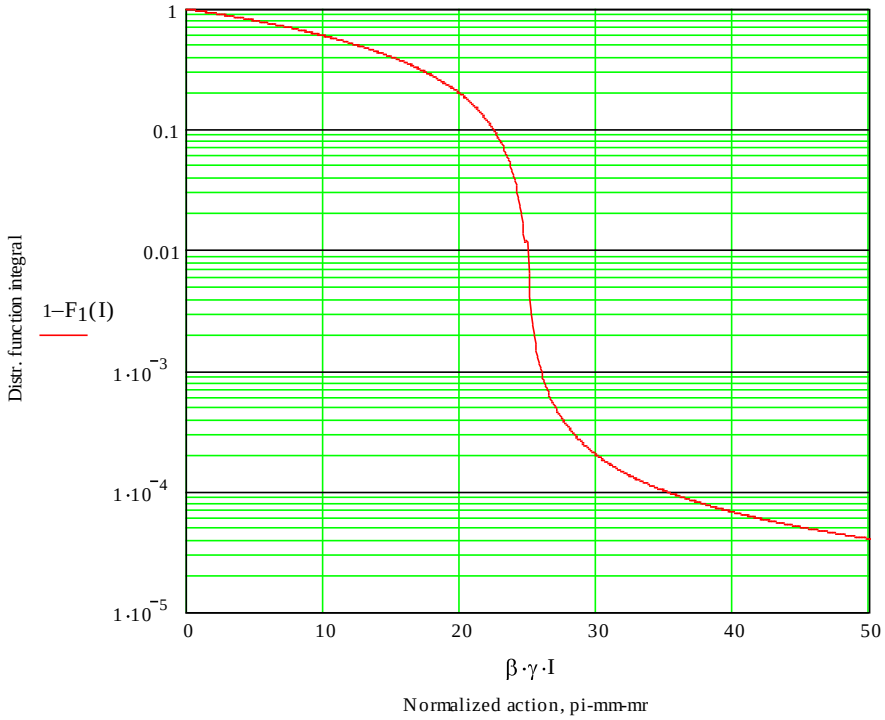

Figure 3.7 The distribution function integral after a single foil passage. The curve represents the number of particles with the betatron action greater than some (given by the horizontal axis).

4 Proton Accumulation in the Recycler

The possibility of injection and storage of high intensity proton beam into the Recycler has been studied. There appears to be no principal limitations from the point of view of accelerator physics if some measures are being taken. The high intensity upgrade does not imply any significant modifications to the machine magnets or vacuum system. The antiproton specific components like the stochastic cooling tanks and the electron cooling section will be removed making the lattice more regular. Major upgrade concerns the RF system where the second harmonic system is added.

Number of particles	1.7×10^{14}
Longitudinal emittance	0.6 eV s
Momentum spread (100%)	$\pm2.5\times10^{-3}$
Transverse emittance (100%) $\varepsilon_h=\varepsilon_v$	25 π mm·mrad
Harmonic number	588
Number of bunches	548
Main RF Frequency	52.811 MHz
Main RF Voltage	750 kV
Second Harmonic RF Voltage	375 kV
Betatron tunes Q_h/Q_v	20.45/20.46
Betatron tune chromaticity	-20
Synchrotron tune (maximum)	0.0067
Transverse acceptance	40 π mm·mrad
Momentum acceptance	$\pm3.2\times10^{-3}$

Table 4.1 Recycler parameters

4.1 Injection

Phase space painting needs to be utilized in order to minimize the phase space density and mitigate the space charge effects. Also, some of the 325 MHz linac bunches have to be chopped for injection into 53 MHz Recycler RF buckets. Below we consider both the transverse and the longitudinal painting.

4.1.1 Longitudinal Painting

The linac bunches sit in every fourth 1300 MHz RF bucket which makes 6.15 bunches per Recycler bucket at 52.8 MHz. The longitudinal painting implies chopping linac bunches which deviate by more than $T_{hgap}=\pm2/6$ of the bucket size from the bucket center. This leaves 4 bunches per RF bucket in Recycler per turn and 356 bunches per bucket per 1 ms linac pulse. Besides the natural spread of phases of the injected linac bunches due to non-integer ratio of the linac and Recycler RF frequencies, we utilize second harmonic RF system and linac energy sweeping to achieve more uniform longitudinal density. The second harmonic RF at the amplitude of half the main RF voltage produces a 100% synchrotron tune spread. When the energy of linac bunches is changed by 18 MeV (2.2×10^{-3}) during the 1 ms pulse the achieved bunching factor is 2.2 and the resulting density distribution is shown in Figure 4.1.

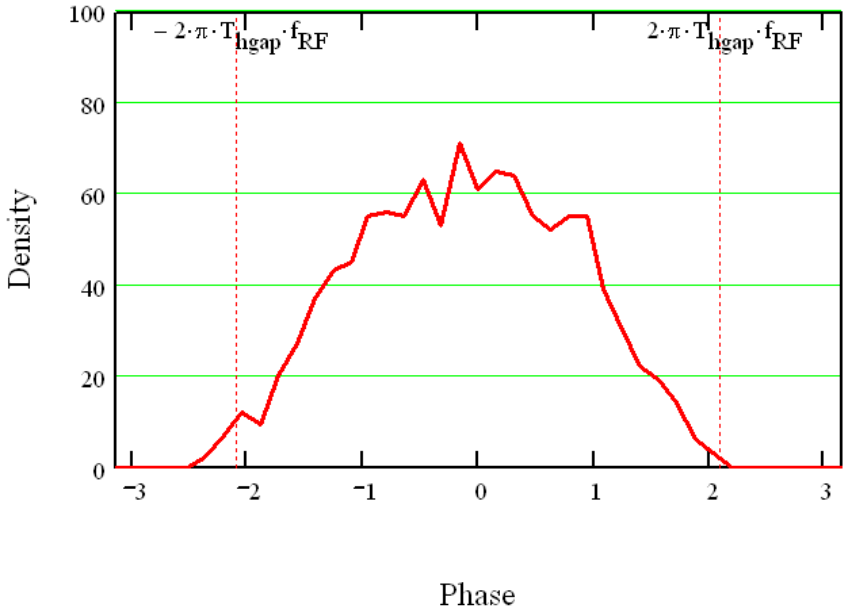

Figure 4.1 Longitudinal phase space density after painting at injection.

4.1.2 Transverse Painting

The best result in terms of minimization of the space charge tune shift is achieved in the case of Kapchinsky-Vladimirsky distribution. Implementation of such a distribution by means of varying the horizontal position and vertical angle of the injected bunch has been studied.[20] It was shown that 356 linac bunches with the 95% normalized transverse emittance of 2.5 π mm·mrad can be painted to create the K-V beam with 100% emittance of 25 π mm·mrad. The assumed Recycler acceptance is 40/40 π mm·mrad which is sufficient to accommodate the injected beam.

4.2 Beam Loss Management and Radiation Protection in the Recycler and Main Injector

Operation of accelerator and beam transport lines at significantly higher beam power envisioned for this project presents some new challenges. Extrapolation of the methods used at Fermilab to design existing, relatively low power accelerators will be not sufficient. Fortunately, techniques developed at megawatt power accelerators such as SNS can be readily applied to this project. Such techniques are already being applied at Fermilab to enhance operation of existing accelerators and beam transport lines. It will be shown that radiation protection can be realized for this project through the straight-forward process of beam loss management.

There are two basic requirements for radiation protection which must be observed. First are the regulatory requirements from the Code of Federal Regulations, DOE Orders, and the State of Illinois which are enumerated in the Fermilab Radiological Controls Manual (FRCM). These requirements are related to health and safety of workers, the public, and the environment. Second are the practical machine control requirements which are necessary to protect machines from short term and long term damage due to beam loss. Prevention of excessive losses improves machine reliability, reduces the frequency of breakdowns, and simplifies required maintenance due to the need for less complex radiation protection procedures. While the methods for achieving these radiation protection requirements are overlapping, the requirements for personnel and environment protection methods tend to be more rigorous and prescriptive than

those required for meeting machine protection requirements. Controls designed primarily for machine protection may not be sufficiently rigorous for personnel and environmental protection.

The Beam Loss Management Goals for this project are listed in Table 4.2 and represent the peak acceptable uncontrolled losses. Uncontrolled losses are defined as those losses that may occur after beam passes through a collimation system. The average uncontrolled losses for the project are a factor of five less than the peak losses. The Design Controlled Losses are estimated at 1.0% of total beam power for the Linac, Recycler, and 8 GeV transport lines The Design Controlled Losses are estimated at 0.1% of total beam power for the Main Injector and the related downstream transport lines. These goals are rigorous but should be achievable using methods described in the following sections.

Beam Energy (GeV)	Beam Power	Protons/second	Region Type	Peak Acceptable Uncontrolled Losses (Watts/m)	Peak Acceptable Uncontrolled Losses (protons/m/sec)	Estimated Percent of Controlled Beam Power Loss	Design Controlled Losses (KW)
8	153 KW	1.2e14	Beam pipe	0.25	1.95e8	NA	NA
8	153 KW	1.2e14	Magnet	3 to 10	2.34e9 to 7.81e9	1%	1.5
120	2.3 MW	1.2e14	Beam Pipe	0.25	1.3e7	NA	NA
120	2.3 MW	1.2e14	Magnet	3 to 10	1.56e8 to 5.21e8	0.1%	2.3 KW

Table 4.2 Beam Loss Management Goals

4.2.1 Use of collimation systems to control beam losses

Collimation systems are a fundamental requirement for high power accelerators, beam transport lines, and the ion stripping injection region used in this project. Multiple stage collimation systems are designed and strategically placed to remove beam halo in controlled, shielded locations. With proper optics and orbit control following collimation systems, beam losses in accelerators, in transport lines and at injection/extraction regions becomes relatively lossless permitting high power operation in conjunction with a relatively safe working environment for beam enclosure, maintenance related activities. Collimation systems are planned for the 8 GeV transfer line just downstream of the 8 GeV linac and the Main Injector accelerator. An H- stripping foil/collimation system will also be included at Recycler Ring injection system. Collimation systems must be designed with shielding to allow personnel access for maintenance and to prevent excessive air, ground and surface water activation. These systems must also be sufficiently shielded to limit radiation losses on the shielding berm surface to levels allowed by the FRCM. While collimation systems are designed to meet machine protection requirements, they provide intrinsic radiation protection necessary for feasible operation of high power accelerators and beam lines.

4.2.2 Residual radiation levels in tunnels

Residual radiation levels in beam transport lines and accelerators due to operational beam losses must be controlled in order to conduct maintenance activities while keeping personnel

radiation exposure as low as reasonably achievable (ALARA). The peak acceptable uncontrolled beam power losses listed in Table 4.2 result in a radiation dose rate of 100 mrem/hr at a distance of 30 cm from the component (beam tube or magnet) surface. The average dose rate at 30 cm from all components should be a factor of 5 lower or 20 mrem/hr at 30 cm. Collimation systems are expected to receive normal beam losses and can therefore be designed to keep radiation exposures ALARA with resulting radiation dose rates less than expected peak dose rates for uncontrolled losses.

4.2.3 Accelerator component activation

Beam loss must be managed in order to limit radiation damage to accelerator and beam transport line components. Based upon Fermilab operating experience with the Booster, Main Ring, Main Injector, and various beam transport lines, observation of acceptable beam losses in Table 4.2 will not lead to radiation damage concerns for accelerator magnet and cable systems.

4.2.4 Electronic berm

High power accelerators and beam lines are capable of producing significant radiological issues including prompt radiation exposure through shielding, prompt radiation damage, equipment damage, air activation, surface and ground water activation, and high residual activation which can lead to excessive personnel exposure for maintenance operations. It is impractical to use shielding alone to mitigate the consequences of prolonged high power beam loss for these various radiological problems. Very thick shields outside of beam enclosures leads to higher excavation and construction costs. Very thick shields inside the tunnel complicate maintenance tasks and require significant oversight to manage and control shielding configurations. Passive shielding can not prevent significant prompt radiation damage such as vacuum loss due to beam tube damage caused by mis-steering. It is therefore important to promptly turn off high power accelerators in the event high power beam loss occurs. Electronic berms [1] (e-berms) can serve to limit the magnitude and duration of high power beam loss.

Electronic berm is a safety system that can be used to meet the regulatory requirements for this project. By comparing beam intensity signals measured, for example, by toroids, the electronic berm can detect a high power beam loss and inhibit further operation of the machine in one Main Injector machine cycle (less than 2 seconds). The cause of the beam loss can be investigated and corrected before injecting additional high beam power pulses thereby mitigating the undesirable effects of prolonged high power beam loss. The electronic berm will be capable of detecting <2% per pulse beam loss. Due to the recovery time in machine operation following a radiation safety system trip induced by the e-berm, high power beam loss can be limited to < 1%. While there are no operational e-berm systems at Fermilab at this time, there is an on-going, low-level effort to develop the e-berm. The e-berm system is a technically feasible safety system that can be readily used for this project.

4.2.5 Prompt radiation shielding

Radiation shielding for an 8 GeV Linac and a new 8 GeV Transport line to the Recycler has been designed for a 480 KW Linac in the Proton Driver project. This shield is designed for a maximum dose rate of 1 mrem/hr for the accident condition and 0.05 mrem/hr for normal conditions. The design for can be readily modified for a 153 KW 8 GeV Linac and Transport line of the Project X..

The existing Recycler Ring/Main Injector beam enclosure has a minimum of shielding thickness of 24.5 feet. To limit the maximum accident radiation dose rate to 1 mrem/hr and the normal condition dose rate to 0.05 mrem/hr, the beam power loss at a point for these two conditions is considered in Table 4.3.

Machine/region	Normal conditions Protons per hour	Normal Conditions Watts/meter	Percentage of full beam power - normal	Accident Conditions Protons per hour	Accident Conditions Watts/meter	Percentage of full beam power - accident
Recycler Ring/beam tube	1.25e16	4,440	2.9%	2.5e17	88,900	58%
Recycler Ring/magnet	2.4e15	850	0.6%	4.8e16	17,100	11%
Main Injector/beam tube	4.5e16	240,000	10.4%	9e17	4,800,000	210%
Main Injector/magnet	8.75e15	46,670	2%	1.75e17	933,000	41%

Table 4.3 Local beam power loss limits for normal and accident conditions

Comparison of Table 4.2 and Table 4.3 illustrates that control of acceptable losses for the purpose of radiation exposure control inside the beam enclosure for maintenance is the limiting condition. The limiting case for the Recycler/Main Injector shielding is for the normal loss condition on Recycler Ring magnets. A normal loss condition of 0.6% beam at a point could lead to a dose rate in excess of 0.05 mrem/hr under normal conditions. Since the e-berm safety system may only reliably detect a 2% beam loss, it would be possible to exceed 0.05 mrem/hr due to beam loss on a Recycler Ring magnet. With an appropriately designed collimation system, it is very unlikely that uncontrolled losses of this magnitude could be lost at a single point. In any case, the FRCM offers alternative solutions for normal conditions above 0.05 mrem/hr, so this is not fundamental concern for the realization of this project. The existing radiation shielding for the Recycler/Main Injection should be acceptable as is if an e-berm Safety System is employed to limit radiation losses between the end of the 8 GeV Linac and Main Injector extraction regions

4.2.6 Machine protection

High power operation of accelerator and associated beam lines can be significantly interrupted under some easily achievable conditions. For example, the undetected failure of a bending magnet power supply could lead to unintentional loss of beam in a beam line or accelerator component resulting in loss of vacuum. Depending on the nature and extent of the damage, accelerator operation can be interrupted for periods of from hours, weeks or months. The high beam power accelerator and beam transport lines will require a machine scheme which promptly disables beam from the 8 GeV Linac in the event an accelerator or beam line component parameter go out of tolerance. Fermilab machine protection system schemes exist which can be used for basic machine protection.

4.2.7 Surface and ground water activation and air activation

Surface water, ground water, and air activation have been studied for the existing Recycler/Main Injector rings. Scaling from existing conditions and assuming the use of additional controls to limit uncontrolled losses in the Recycler and Main Injector machines, the surface water activation, ground water activation and air activation should remain well within acceptable limits.

4.3 Particle Losses and Radiation

4.3.1 Beam Halo and Losses

Provided that there is no instability driving the emittance growth, formation of the distribution tails and particle losses will be dominated by two processes:

a) single Coulomb scattering on the foil

b) scattering on the residual gas.

The estimated number of particles beyond the 40 π mm·mrad acceptance after 5 passages through the foil is 4×10^{-4}. This corresponds to the power of 130W which should be handled by the collimation system.

The second process due to the high Recycler vacuum (~10^{-10} torr) is very weak. The achieved beam life time of ~1000 hours corresponds to the total loss rate of 3×10^{7} protons/s or average power of 0.04W.

4.3.2 Radiation Resistance of the Recycler Permanent Magnets

Permanent magnets built using strontium ferrite bricks have been tested for stability against demagnetization under various conditions.[21,22,23,24] A total of ten test dipoles were built to monitor ferrite behavior under a variety of stressing conditions, including irradiation, mechanical shock, extreme thermal excursions, and long term magnetization stability. These test magnets were geometrically similar to, but much shorter than, the magnets built for the 8 GeV transfer line at FNAL. During these tests, no loss of magnetization was observed for bricks exposed to a proton beam, and a magnet exposed to several Gigarads of Co_{60} gamma radiation suffered no measurable demagnetization. In another test a magnet was irradiated by a source putting out 0.8 Mrad/hour for 268 hours. The observed change in magnetic field was about .5 Gauss out of 1465 Gauss, or ~2 $X10^{-4}$ which is within of allowed variations.

4.4 Coherent Stability in RR and MI

In principle, there are two sorts of transverse coherent instabilities in RR and MI: due to resistive wall and due to electron cloud (assuming that Lambertson magnets in MI are going to be shielded or replaced). The problem of coherent stability is most pronounced at injection energy; the small gamma-transition jump at MI is assumed. All essential details of the resistive-wall instability are well predicted. On the contrary, only rough estimations can be presented for electron cloud. To suppress both instabilities, three means are foreseen:

- Second RF harmonic, providing high (~100%) spread of the synchrotron tunes;
- High chromaticity to provide Landau damping
- Broad-band damper.

Resistive wall instability is the fastest at the lowest frequency, related to the fractional tune: its e-fold growth time is calculated as 10 turns. The same growth time is estimated for e-p instability,

assuming 20% charge compensation, evenly distributed within the cylinder of 2.5 cm radius. The most unstable mode for e-p instability is estimated at ~10-50 MHz. To suppress both instabilities, the chromatic tune spread has to exceed space charge tune separation between the coherent and incoherent lines. The latter value is calculated as vertical/horizontal = -0.04/-0.03 (no e-cloud) or -0.03/-0.08 for (20% charge compensation). The full energy spread at injection is 0.25%; thus, to cover 0.04 of the space charge tune separation, the chromaticity has to be -16. To keep the e-cloud density below 20%, bunch structuring (making some buckets empty), surface coating and conditioning can be applied. Although there is some uncertainty with the e-cloud, a positive experience of B-factories at similar parameters gives a good hope to overcome this problem. In view of the e-cloud uncertainty, a broad band damper up to 50-200 MHz has to be foreseen.

Longitudinal instability should not be an issue: at injection, the energy spread is ~ 20 times above the threshold.

5 Acceleration in the Main Injector

5.1 Main Parameters

The main injector upgrade increases the total beam power by almost an order of magnitude. As one can see from Table 5.1 it is achieved by 5-fold increase in number of particles accelerated in one cycle and shortening magnetic cycle from 2.2 s to 1.4 s. There appears to be no principal accelerator physics limitations on machine parameters. The upgrade does not imply any significant modifications to the machine magnets or vacuum system. To minimize the machine impedance the existing Lambertson septum magnets have to be shielded similar to the Tevatron injection Lambertson magnet. The larger beam power will require significant upgrade of the existing RF system; and the larger beam current will require building more powerful transverse damper.

Parameter	Present	MI upgrade
Injection kinetic energy, GeV	8	
Extraction kinetic energy, GeV	120	
Circumference, m	3319.42	
Revolution frequency at injection, kHz	89.815	
γ– transition, γ	21.62	21.62
γ-transition jump, $\Delta\gamma$	-	2
Cycle duration, s	2.2	1.4
Total number of particles	$3.4\cdot10^{13}$	$1.7\cdot10^{14}$
Beam current at injection, A	0.49	2.45
Betatron tunes, Qx/Qy	26.42/25.41	26.45/25.46
Normalized 95% emittance, mm mrad	15/15	25/25 [1]
Norm. acceptance at injection, mm mrad	40/40	40/40
90% longitudinal emittance, eV s	0.4	0.5
Maximum space charge tune shifts, ΔQx/ΔQy	0.033/0.038	0.043/0.046
Number of bunches	480	548
Number of particles per bunch	$7\cdot10^{10}$ ($9\cdot10^{10}$) [2]	$3.1\cdot10^{11}$
Betatron tune chromaticity	?	-20 - 20
Abort gap, μs	1.6	0.7
Maximum power intercepted by collimation system, kW	<1.6	<1.6
Average beam power on the target, MW	0.3	2.3

Table 5.1 Main Parameters of Main Injector

Direct multi-turn injection of linac beam into Recycler with consecutive beam transfer to MI allows one to have additional advantages which cannot be implemented in other schemes. First, the beam chopping at low energy in the linac allows one, if necessary, to leave only one

[1] KV distribution is implied

[2] Population of slip-stacked bunches for antiproton production

abort gap which minimizes the bunch population. This is considered to be a main scenario. Nevertheless, if necessary a special bunch structure can be created by chopping linac beam at small energy. It can be helpful in suppression of the electron multipactoring by proton beam and, consequently, *ep*-instability. Second, painting small emittance of linac beam allows into Recycler allows one to make a flat density distribution.[25] The distribution can be quite close to the desired KV—distribution. That reduces the space charge tune shifts by factor of 3 relative to the Gaussian beam with the same 95% emittance. This reduction is taken into account in Table 5.1 for MI upgrade.

The injection and extraction kickers need to be modified so that they could operate with 10 μs batch length. The abort gap of 0.7 μs was chosen to minimize technical risks associated with the fast rise time of the extraction kicker voltage and the fast fall time for injector kicker. If necessary the injection kicker can be supplemented by bumper kickers to minimize betatron oscillations in the bunch tails. Presently, the MI acceptance is limited by extraction Lambertson magnets to about 80 mm mrad. Acceptance of 40 mm mrad is assumed for the upgrade leaving ~6 mm for steering errors.

The MI upgrade uses the same RF frequency as present MI. To reduce the peak longitudinal density the second harmonic RF system is used. Its amplitude and phase are chosen to zero linear and quadratic terms of RF force in the bunch center:

$$V(\phi,\phi_0) = V_0\left(\sin(\phi) - \frac{\cos(\phi_0)}{2}\sin\left(2(\phi-\phi_0)\right) - \frac{\sin(\phi_0)}{4}\cos\left(2(\phi-\phi_0)\right) - \frac{3}{4}\sin(\phi_0)\right) \qquad (5.1)$$

where ϕ is the particle phase and ϕ_0 is the accelerating phase. Such choice reduces the longitudinal density by ~15% but what is even more important it introduces large synchrotron tune spread helping to suppress instabilities. Table 5.2 and Table 5.3 present the main parameters of the first and second harmonic RF systems. Figure 5.1, Figure 5.2 and Figure 5.3 present the MI magnetic cycle and dependence of RF and beam parameters on the acceleration time. The dependence of RF voltage on time is chosen so that to keep bunch as long as possible through entire accelerating cycle. The second harmonic RF makes a flat bottom of potential well and therefore synchrotron frequency is zero at zero amplitude. At small amplitudes it grows linearly with amplitude and achieves its maximum at amplitudes of more or about 82% (depending on the accelerating phase) of the bucket size. Figure 5.3 presents a dependence of this maximum frequency on the acceleration time.

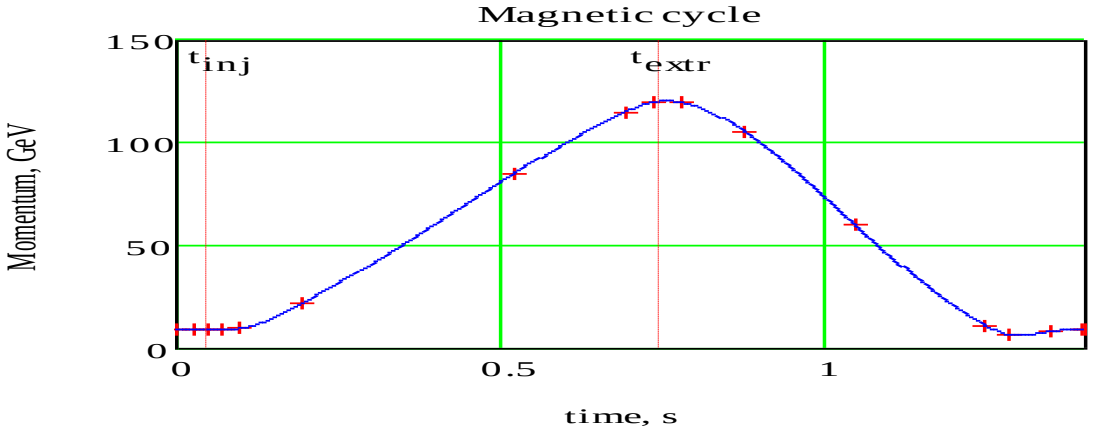

Figure 5.1 Dependence of beam momentum on time during MI magnetic cycle

	Present	MI upgrade
Harmonic number	588	
Frequency swing from injection to extraction, MHz	52.811 - 53.103	
Number of cavities	18	18
Shunt impedance per cavity, (R/Q)*Q, kΩ	500	100
Loaded Q	4000	4000
Maximum operating parameters		
RF voltage, MV	4.2	4.2
Peak RF power, MW	3.2	13
Average RF power, MW	0.8	5
Operating parameters required by the presented accelerating scenario		
RF voltage, MV		3.43
Maximum RF power, MW		10.59
Maximum power transferred to the beam, MW		7.32
Maximum power lost in the cavity walls, MW		3.27
Average RF power, MW		4.1

Table 5.2 Parameters of the first harmonic RF system.

	Present	MI upgrade
Frequency swing from injection to extraction, MHz	105.622 - 106.206	
Number of cavities		5
Shunt impedance per cavity, (R/Q)*Q, kΩ		100
Loaded Q		4000
Maximum operating parameters		
RF voltage, MV		1.2
Peak RF power, MW		1.5
Average RF power, MW		0.9
Operating parameters required by presented accelerating scenario		
RF voltage, MV		1.16
Maximum RF power, MW		1.34
Maximum power transferred to the beam[3], MW		-1.83
Maximum power lost in the cavity walls, MW		1.34

Table 5.3 Parameters of the second harmonic RF system

Coherent beam stability is similar for MI and Recycler and is discussed in the Recycler section. While the transverse beam stability is mainly achieved by using large chromaticities (similar to the present Booster operation) we also plan to increase power of the existing damper so that the damper could damp injection oscillations of about 0.5 mm amplitude within ~10 turns.

[3] As one can see from the Eq. (1) the second harmonic is phased so that it decelerates the beam proportionally to $V_0 \sin(\phi/4$. Therefore the beam pumps energy into the cavity and the power transferred to the beam is negative.

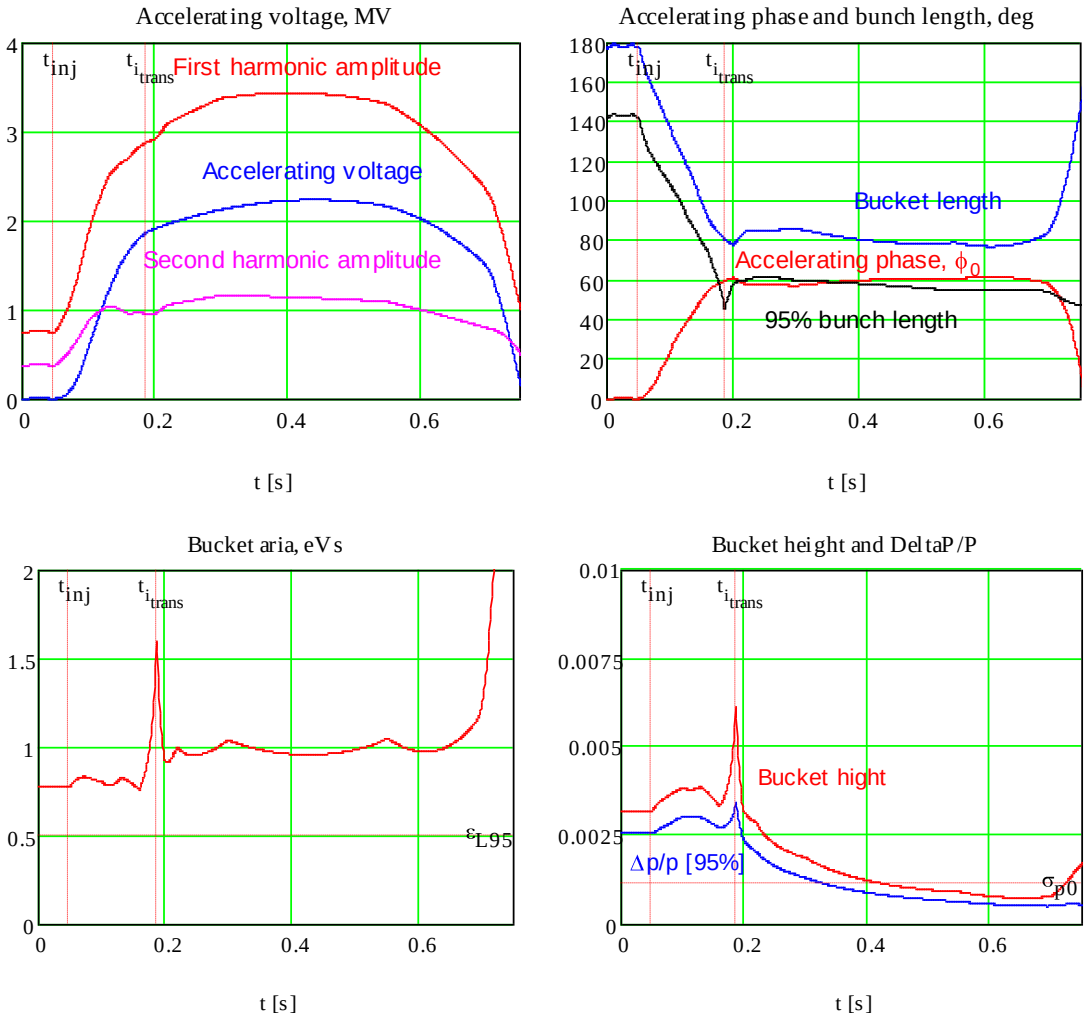

Figure 5.2 Dependence of RF and bunch parameters on time; top left: red - 1-st harmonic voltage, blue accelerating voltage, magenta – 2-nd harmonic voltage; top right: red – acc. phase, blue – bucket length, black – 95% bunch length; bottom left: bucket area; bottom right: red – bucket height, blue – 95% Δp/p.

Figure 5.3 also presents dependences of the incoherent betatron tune shifts on the acceleration time. They consist of two contributions. The space charge tune shifts which is amplitude dependent and therefore cannot be compensated[4]; and the tune shifts due to interaction with flat vacuum chamber and magnetic core of dipole magnets (the charge reflection in vacuum chamber walls, and the beam DC current reflections in the cores of dipoles). For ultra-relativistic beam the second contribution practically does not depend on amplitudes of betatron and synchrotron motion and therefore can be corrected by tune offsets proportional the DC beam current. We already do this for present MI operation. As one can see from Table 5.1, the flattened distribution and increased emittances allowed us to have the space charge tune shifts only slightly above present values. The chosen values of the space charge tune shifts should not

[4] There are a few ideas how this could be done but they have not achieved a state of maturity required by the project of this scale.

present a serious challenge for the future MI operation.

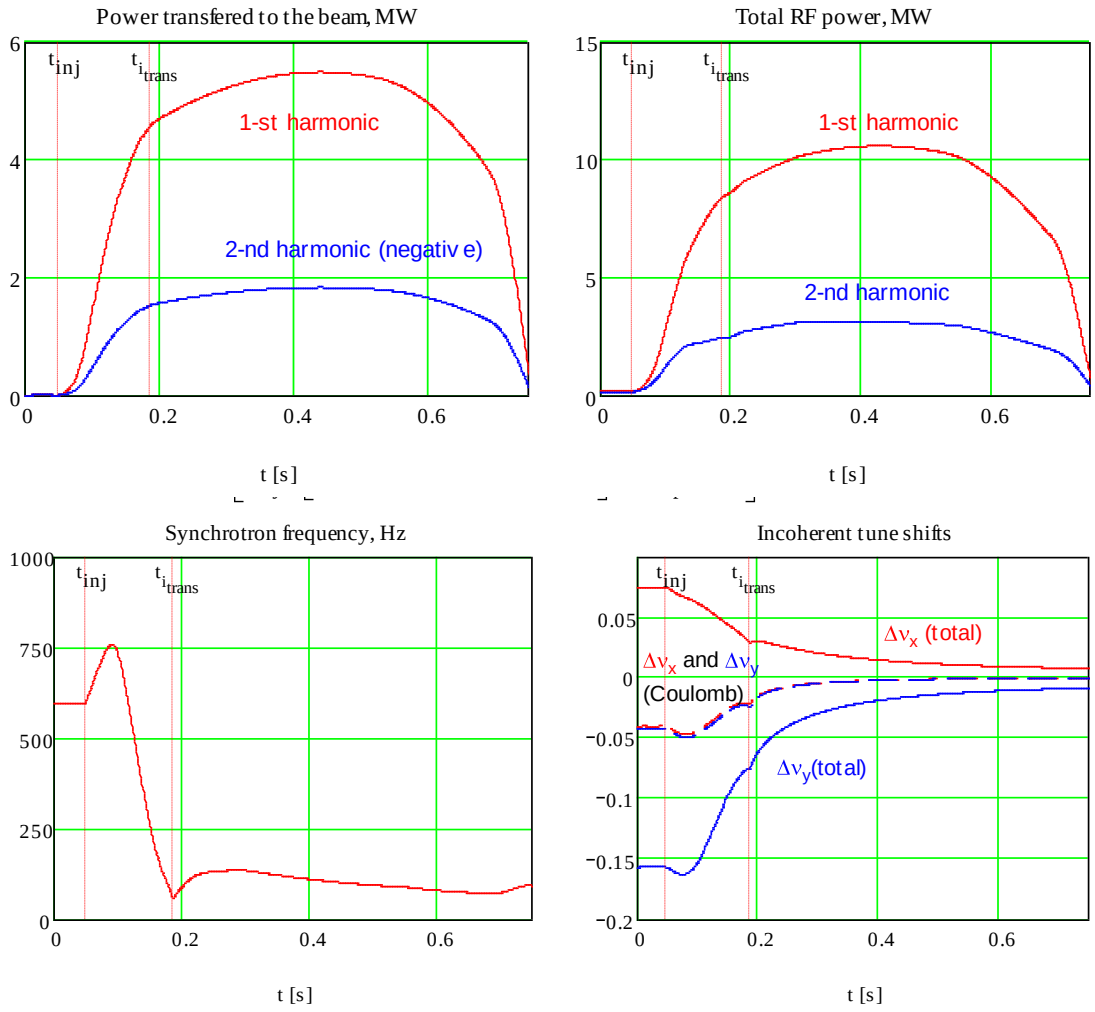

Figure 5.3 Dependence of RF power, maximum synchrotron frequency and incoherent tune shifts on the accelerating time.

5.2 Transition crossing

The γ_t-jump is used to minimize longitudinal and transverse emittance growths excited by the transition crossing. The conceptual design of a first order gamma-t system consists of 8 sets of pulsed quadrupole triplets.[26] It provides a $\Delta\gamma\tau$ from 1 to -1 within 0.5 ms *i.e.* transition is crossed 20 times faster than the normal ramp. Note also that the maximum synchrotron frequency at transition is 57 Hz resulting in 10 deg. synchrotron phase advance during transition.

The design uses a first-order system, making use of the dispersion free straight sections in the MI lattice. Each triplet has two quads in the arc and one of twice integrated strength in the straight section, with a phase advance of π between each quad. The main advantage of such a design is that the perturbation to the original lattice is localized. The dispersion wave is localized between the two arc quads and the beta-wave is localized between each cell.

As one can see from Figure 5.2 in the case of γ_t-jump of 2 units the beam never becomes too short. Even at transition the beam space charge longitudinal field is almost 2 orders of

magnitude smaller than the RF fields and in the most of cases can be neglected. That should allow transition crossing with no beam loss and negligible longitudinal emittance growth. Results of simulations verifying it are presented in Figure 5.4. The simulations were carried out with ESME for 0.4 eV-sec longitudinal emittance per bunch, and $3.2 \cdot 10^{11}$ particles. Without jump the $\Delta p/p$ reaches 1.2% at transition and exceeds the momentum aperture of MI. The longitudinal emittance blow-up at transition without the jump is 80% compared to 8% with the jump. Estimates show that accounting the second harmonic accelerating voltage neglected in these simulations makes the transition more adiabatic and less susceptible to the longitudinal instabilities.

5.3 RF System

The peak power transferred to the beam from RF system is 5.5 MW. As one can see from Eq. (1) the requirement of flat RF bucket results in that the second harmonic RF system decelerates the beam thus requiring larger power of the first harmonic RF. Partially it is compensated by smaller voltage of the first harmonic system originated from larger RF bucket size for the fixed voltage. Presently, we consider scenario where the amplitude and phase of the second RF harmonic are chosen to make the flat bottom of the potential well. In the future we can consider an intermediate scenario where we start acceleration with the flat potential well to minimize space charge effects at the injection, and then one can reduce amplitude of the second harmonic in the course of the acceleration. An advantage of such scheme is that it would allow reducing the power of the first harmonic RF system but it would also reduce a margin of beam stability.

The number of RF cavities is limited by available space and their total longitudinal impedance. The chosen number of cavities requires RF power sources capable of delivering more than 700 kW/cavity. Fortunately in the 50 - 100 MHz frequency range, two high power tetrodes (EIMAC 8973 and Thales 526) with output powers and plate dissipations in excess of 1 MW are commercially available. Either of these tetrodes could be used in the final amplifier stage and be driven by one of the existing MIRF power amplifiers. The final amplifier stage would be located in the tunnel as close as possible to a new low R/Q (25 ohm) RF cavity. Depending on the final design parameters for the 2^{nd} harmonic RF system, the Thales TH628 diacrode might be an attractive alternative at the higher frequency.

5.4 Beam Loss and its Localizing

Painting the beam in MI in three degrees of freedom in Recycler is expected to be extremely helpful in reducing the beam loss in MI. Nevertheless an accurate beam loss estimate is extremely complicated; and this multidimensional problem cannot be fully assessed before machine will be operating. The following mechanisms contribute to the beam loss during beam operations: scattering on the residual gas atoms, Touschek effect, loosing beam tails at injection and extraction, beam loss due to instabilities, beam loss excited by non-linear resonances (including resonances excited by the beam space charge), and beam loss due to errors in operations.

For present MI vacuum of $\sim 10^{-7}$ Torr the beam loss due to scattering on the residual gas atoms is about $3 \cdot 10^{-4}$ per cycle resulting in the power loss of ~150 W. This is not a negligible number. Consequently, we need to anticipate that in the future high power operations the vacuum cannot be worse than present. It is expected that at the beginning of high power operations we will have strong multipactoring excited by the beam space charge. It will strongly affect vacuum,

and vacuum system has to have enough capacity to take this additional load. Beam loss due to intrabeam scattering and Touschek effect is expected to be below 10^{-5} and can be neglected.

Machine parameters are chosen so that to avoid problems with instabilities and non-linear resonances. It is expected that in normal operations they should not make significant contribution to the beam loss. Multipactoring of electrons and related with it *ep*-instability are expected to be the major offenders. Successful operation of B-factories in SLAC and KEK with close positron beam current, bunch frequency and energy is may be the best prove that the problem is solvable. Their experience says that conditioning of vacuum chamber walls is a major remedy. Making such conditioning sufficiently fast implies an operation on the maximum power and significant beam loss. Presently, we believe that the mentioned already remedies to mitigate the *ep*-instability are sufficient but more detailed studies are required. If necessary, TiN coating and/or clearing electrodes can be used.

Taking into account complicated reality of 24 hour machine operation it would be prudent to expect the beam loss of about 0.1-0.2% resulting the beam power loss of 1-2 kW. This efficiency is more than an order of magnitude less than the present MI efficiency and will not be easy to achieve at the beginning of machine operation. MI collimation system to be installed during 2007 shutdown is capable of intercepting 1.5 kW beam loss power. More detailed studies are required to understand if this power is adequate or needs to be increased. It is expected that in normal operations this system will be intercepting major fraction of the beam loss (>99%) leaving the rest of the tunnel comparatively clean.

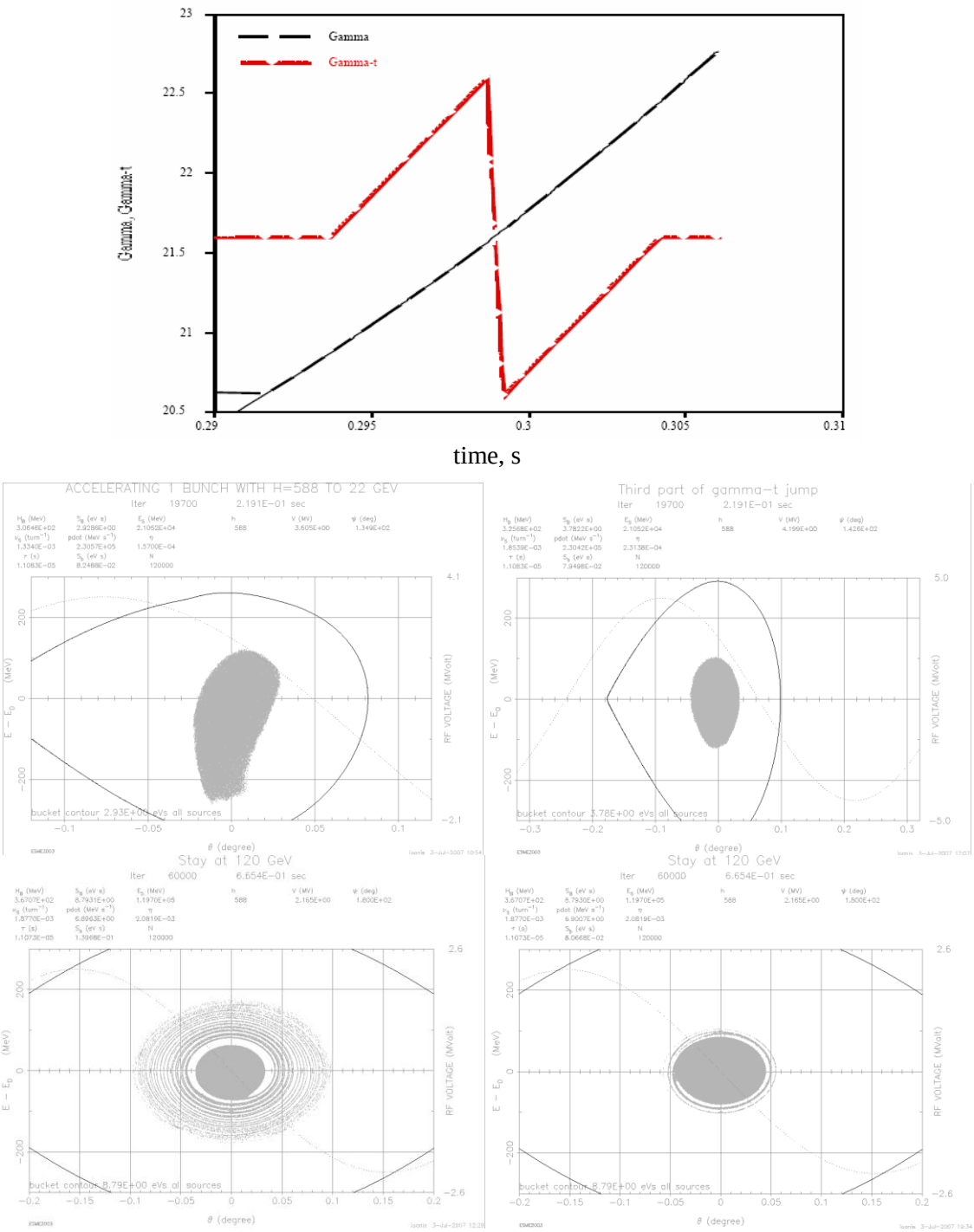

Figure 5.4 Results of ESME simulations of γ_t-jump; top – dependence of γ on time, center - phase space right after transition with (right) and without (left) a γ_t-jump, bottom - phase space at 120 GeV with (right) and without (left) a γ_t-jump.

6 8 GeV Extraction from the Recycler

6.1 Options for beam extraction from the Recycler

In addition to providing 2.3 MW beam power at 120 GeV/c for the neutrino program (1.7E14 protons/1.4 sec), there are 4 empty linac cycles which could be used for other purposes while the MI is ramping. The current vision is that the beam is injected into the Recycler in formed 53 MHz buckets in the Recycler. It is assumed that the linac current is constant at 9 mA. A 700 ns abort gap is preserved in the Recycler which gives about 5E13 injected during the 1 ms beam pulse each linac cycle with the beam bunched in 53 MHz.

Either fast or resonant extraction techniques are considered. Fast extractions involve kicking some fraction of the beam, from one bunch to the full ring, out in a single turn. Variations in bunch structure are simply controlled with the 325 MHz beam chopper. Resonant extraction implies a much smaller instantaneous intensity and the spill duration may range from 200 to 800 ms.

There are two locations where one might think of locating an extraction system that would transport beam from the Recycler to some experiment. The first location under consideration is the 52 region where the Main Injector currently extracts beam into the P1 line for transport to/from the Pbar Source, the Tevatron, and Switchyard. The extraction system could be installed in the Recycler immediately above the MI system which would then connect with the P1 line which could transport beam to the Pbar Source. The extraction system design is dependent on which type of extractions are utilized. A conceptual design of a sub-transfer line which connects the Recycler to the P1 line which uses the Recycler as a partial turn transfer line has been published.[27]

An alternative location which might be considered is the 40 region where both the MI and Recycler abort extraction systems are located. Both the Main Injector and Recycler share the same abort absorber. The current MI abort absorber was designed with a bypass aperture through the absorber for transport of beam to a "green field" experimental hall. This feature has never been used to date. An extraction kicker for full turn or batch by batch already exists at the proper location. A dipole in the abort line would alter the trajectory from the absorber to the bypass.

Beam requirements for a particular experiment will determine which of the extraction techniques and locations are chosen. Currently, a mu-2-electron conversion experiment is being discussed. The current version of the experiment being discussed would like short proton bunches, < 30 ns, on the target separated by about 1.6 us. They would like 10^{-9} extinction between bunches. The bunch intensity is on the order of a few 10^{8} per bunch.

6.2 Recycler resonant extraction

The current Recycler lattice generally mirrors the MI lattice design, particularly in the Nova era when the electron cooling straight section is replaced by a FODO lattice. Since resonant extraction is currently accomplished in the MI, no major global lattice reconfiguration is anticipated to be required for resonant extraction. A new injection straight section, however, is envisioned at 10 where the FODO lattice is replaced with a symmetric straight section to facilitate multi-turn H- injection. This modification has been proposed for Main Injector[28] and could be implemented in the Recycler.

The Recycler is composed of permanent magnet gradient magnets and quads, so any lattice change would require modification and/or addition of permanent magnets. Electromagnet quads are installed in the 60 straight section in five families to produce a localized phase trombone for tune control . This means that the phase advance throughout the rest of the ring is fixed and only the phase across the 60 straight is modified for tune control. The current tune reach of the phase trombone should allow raising the fractional horizontal tune upwards toward 0.485 for initiation of resonant extraction. Sine and cosine harmonic quad families, utilizing the same design electromagnet quads and consisting of 2 to 4 magnets in each family, would be required for control of the extraction. In addition, the Quad eXtraction Regulation system, consisting of air core quads would need to be either moved from the Main Injector or replicated. To create an amplitude dependent tune shift a set of octupoles are required. A set of 54 ocutpoles, with a strength of $B'''L/\beta\rho \sim 0.418\ m^{-3}$ at 10 amps are installed in the MI. Due to the large octupole content of the MI quads, these circuits are not currently used for resonant extraction. The Recycler gradient magnets has a very small octupole content so a set of octupoles, appropriately placed to generate a 0^{th}- harmonic would be required. These magnets are 13.5 times stronger at 8 GeV than 120 Gev, so there should be ample strength in the these octupoles.

The resonant extraction process relies on being able to bring the base tune as close to the ½ integer stop band as possible and then ramping the beam through the half integer stop band in a controlled fashion. This suggests that a small dp/p and chromaticity are desirable to reduce the tune spread. Current estimates for the space charge tune shift in the Recycler with 1.7×10^{14} protons and a normalized transverse emittance of 25 π-mm-mr in 53 Mhz buckets (bunching factor of ~0.47) is about $\delta_{SC} \sim 0.04$. To stabilize this tune shift, the momentum spread, dp/p, should be 0.4% and the chromaticity should be on the order of -10 units.

It is clear that the closest approach of the base tune to the half integer stop band would be $\delta \sim 0.04$. Based upon MI simulations this would be difficult, if not impossible, to implement. If only a single linac cycle is injected, 5.7×10^{13}, the space charge tune shift is reduced by a factor of three so that the product of the chromaticity and momentum spread could also be reduced by a factor of three, which brings the tune spread closer to a workable value. This would produce a spill with a 53 Mhz bunch structure. Debunching would further reduce the bunching factor and the space charge tune shift, so the momentum spread could be reduced by another factor of ~2, thus producing a uniform spill structure. Any attempt to create greater bunching using barrier buckets, with a single linac pulse, to obtain short 30 ns bunches separated by 1.6 μs, only aggravates the problem as the space charge tune shift increases by a factor of ~ 25 up to $\delta_{SC} \sim 0.33$. Resonant extraction is not possible in this scenario.

A simplified analysis for ½ integer extraction from the Main Injector at 120 GeV[29] was dusted off and used to investigate the more important parameters utilizing some beam parameters specific to the Recycler. For this investigation,[30] the initial tune offset, dp/p, and chromaticity were varied using the MI lattice at 8 GeV/c. Extraction was simulated to extract at MI52 (septa at 520 and Lambertson 522) with the septum wires at -16 mm. The beam and machine parameters were set to 8.89 GeV/c with a dp/p = 0.133% (95%) , transverse emittance of 25 π-mm-mr (95%) and chromaticity in both planes set to -10 units. With such a large tune spread, 0.0133, the base tune could only be raised to 26.475 without losing beam. Three sets of data are shown in Figure 6.1. Keeping the base tune and chromaticity constant, the phase space (both circulating and extraction) for +/-0.155% (98%) and zero are plotted. Every particle in each data set has the same momentum offset. The plot on the left is just following the septa and the plot on the right is

the entrance of the Lambertson. In each curve 1000 particles are tracked. The extraction points are accumulated over the entire cycle, where as the circulating phase space is a snapshot taken half way through the process. Due to the negative chromaticity the low momentum particles come out almost immediately and the plot on the right shows that the position of these particles overlap the high momentum circulating beam, hence no gap between the circulating and extracted beam. Some improvement could be made but the large beam size and large momentum spread make resonant extraction at 8 GeV from either the Main Injector or Recycler a very unattractive option, if at all possible.

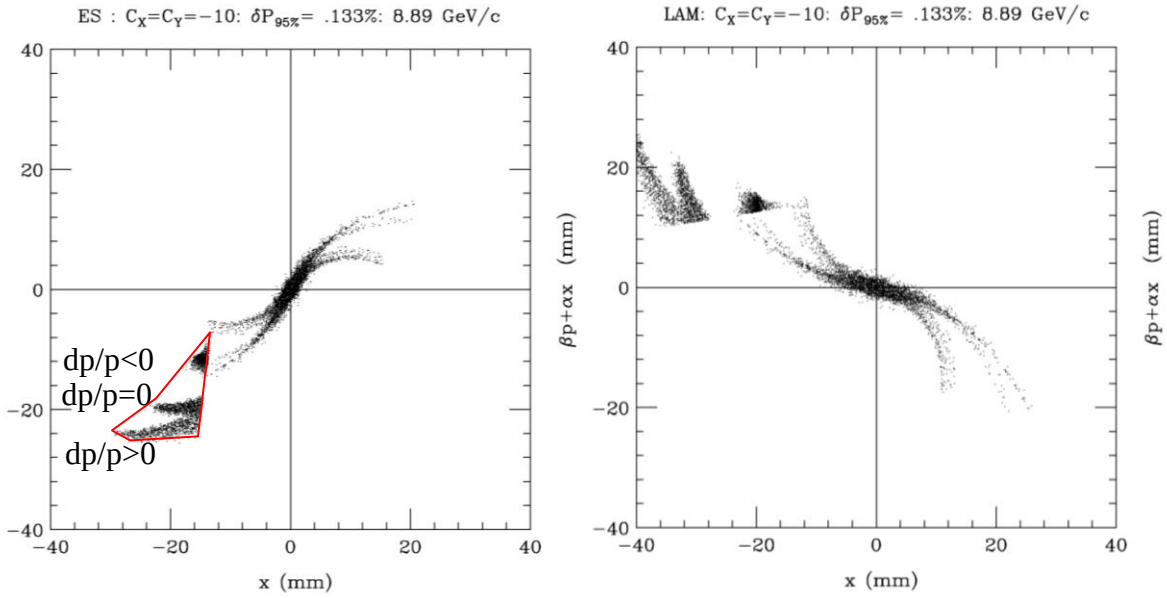

Figure 6.1 Circulating and extracted phase space at 8.9 GeV/c for three values of dp/p.

6.3 Recycler fast extraction

This mode of extraction could utilize the 53 MHz bunch structure. The harmonic number of the Recycler is 588 with a revolution period of 11.13 μs. Typically, an abort gap of 40 buckets (~750 ns) is installed in the beam structure for the rise time of the full turn abort kicker. The details of filling the remainder of the 548 buckets is determined by the fast 325 MHz chopper in the Medium Energy Beam Transport (@2.5 MeV). Several options exist for bunch structure and intensity per extraction. They range from extracting the entire ring (548 bunches) to extracting single bunches. The details of the kicker system required for each of these options are determined by the rise and fall time and flattop length.

For full turn extraction, the rise time should be less that the length of the abort gap or 750 ns. The fall time is unimportant and the flattop needs to be at least 548/588* 11.13 μs or 9.3 μs. Current kicker and power supplies exist which would accommodate this mode of extraction.

Using the chopper to remove beam from 2 or 3 53 MHz buckers every 84 buckets, while maintaining the abort gap, simulates the box car loading final bunch structure. In this mode, single batches made up of 81 53 MHz bunches could be extracted by a kicker with a rise and fall time of 60 ns and flattop length of about 1.3 μs. These kickers are similar in design as those specified for the Nova project.

Painting a longitudinal bunch length of 10-12 ns leaves 6 to 8 ns between 53 MHz bunches The beam is longitudinally painted into 546 bunches. The revolution period of the Recycler is 11.13 microseconds. Six bunches are extracted each turn which takes 90 turns or ~ 1 millisecond to extract all the beam from the Recycler. This would produce intense beam , ~$1x10^{11}$ /bunch with a length of ~ 10-12 ns separated by ~1.6 μs.

To extract a single bunch would require a fast kicker with a rise and fall time of approximately 6 to 8ns and a 10-14 ns flattop with a rep rate of 500 kHz for a millisecond. With advances in switching capabilities of solid-state devices (MOSFETS and GaAsFets) , these devices are being incorporated into high voltage supplies capable of 10's of kilovolt output with few to 10's of nanosecond rise and fall times. These techniques are currently utilized in the barrier bucket modulators and the 325 Mhz chopper (with few kV and few ns rise times) being developed for the HINS project.[31] Modulators with 18 kV output and <10ns rise/fall time have been developed at LLNL which show promise for this application.[32] The extraction procedure would move the beam transversely close to electrostatic septa where the fast kicker would then kick the beam across the ground plane wires. For a 95% normalized emittance of 25 π-mm-mr and a beta of 40 meters, the sigma is roughly 4 mm. Assuming 99% of the beam is contained within 3 sigma, the fast kicker would be required to displace the beam 24 mm across the septa. The septa voltage would then kick the beam into the magnetic Lambertson to complete the extraction process. The magnitude of the fast kick required to move the beam completely across the septa is on the order of 500 microradians. Assuming a plate voltage of 20 kV and a gap of 2 inches it would require roughly 10 meters of kicker to produce the required kick. Increasing the voltage or reducing the required kick angle by reducing the transverse emittance could lower the space requirement. A 2 meter electrostatic septa with a 40 cm gap and 100 kV is sufficient to place the extracted beam in the field region of the Lambertson.

6.4 Debuncher Resonant extraction (for mu2e conversion experiment)

The initial concept for supplying 8 GeV beam to the Pbar Source for a mu2e experiment utilizes the Recycler as a partial turn transfer line (i.e. injection at 10 and extraction at 52) to transfer beam at a 15 Hz rate from Booster through part of the Recycler into the P1 line and ultimately into the Accumulator where several Booster batches are momentum stacked.[27] This requires no RF manipulation in the Recycler.

Assuming the linac operates at 5 Hz and beam is longitudinally painted into 53 MHz bunches, an injection pattern can be envisioned such that several empty buckets can be left between a set of 81 filled buckets such that an extraction kicker of the kind used for Nova injection could kick out 3 batches at a 15 Hz rate each linac pulse length. In this fashion three batches can be momentum stacked in the Accumulator during the linac 5 Hz rep rate. In this scenario the linac would only inject once into the Recycler during the 4 empty cycles not used for MI injection.

An alternate scheme for transferring beam from the Recycler to the Accumulator using multi-turn (6 turns) transverse stacking in the Accumulator[33] has been suggested. The extraction requires a full turn extraction kicker. Details of the Accumulator stacking have not been published.

Both of these scenarios place the dipole extraction (deflection) scheme at 52 in the Recycler with a true extraction system involving a kicker and Lambertson as compared to the scenario already discussed.[27]

It is clear that there are several ways to prepare and extract beam from the Recycler that loads the Pbar Source rings for ultimate resonant extraction from the Debuncher. Several notes have been written on Accumulator momentum stacking with beam from Booster (or Recycler)[34] and rebunching in the Debuncher.[35,36] Several (four to six) Booster batches will be momentum stacked in the Accumulator. These will then be captured in an h=4 RF system, and the beam will be transferred into the Debuncher. Once in the Debuncher, the beam will be captured and phase rotated by an h=1 RF system to produce a single, narrow bunch. Finally, this will be slow extracted to provide the beam structure needed by the mu2e experiment. It could also be single turn extracted to provide beam to other muon experiments.

When the cooling hardware is removed, the straight sections in the Debuncher will allow a great deal of flexibility for the installation of extraction and harmonic hardware. The baseline design currently assumes third integer resonant extraction due to extensive worldwide experience and the fact that the existing tune of the Debuncher is close to the 29/3 resonance. The exact location of the extraction region will depend on the direction chosen for beam rotation and other geometrical considerations, but we will assume that the beam is going in the current direction of reverse protons, in which case a logical extraction point would be to place the electrostatic septum between Q107 and Q106, and the extraction Lambertson between Q105 and Q104. The points just inside the unused ’07 quads are well phased to efficiently drive the third integer resonance.

Detailed modeling of the resonant extraction is under way, but the basic parameters of the resonance are shown in Table 6.1. The septum placement is driven by having the outside of the extraction gap at the limit of the horizontal acceptance. The sextupole strength and tune shift are determined by setting the desired step size to be equal to the gap in the electrostatic septum. The septum and Lambertson parameters are chosen at this point to be similar to those used in the Main Injector. To first order, efficiency is determined by the with of the electrostatic septum plane over the step size. The Main injector septum uses 100 micron wire, so the inefficiency should be on the order of 1%. In practice, it is typically 2%. At the initial design intensity, this would correspond to about 500 W of loss, which is already challenging given the shallow depth of extraction location. This will increase if the linear proton accelerator results in increased total proton flux. More aggressive septum designs, with thinner electrostatic planes and other loss mitigating features are being investigated.

Resonant Extraction Parameters	
Kinetic Energy (GeV)	8
Working tune (ν_x/ν_y)	9.769/9.783
Resonance (ν_x)	29/3
Normalized acceptance (x/y πmm-mr)	285/240
Normalized beam emittance (πmm-mr)	25
β at electrostatic septum (m)	8
β at Lambertson (m)	10
β at harmonic quads (m)	10
Septum gap/step size (mm)	10
Septum field (MV/m)	8
Septum length (m)	3

Table 6.1 Debuncher Resonant Extraction parameters

7 120 GeV Beam for Neutrino Experiments

Two neutrino beam scenarios were considered for 120 GeV beam from the Main Injector:

- A new beam-line/target-hall directed at a new detector at the DUSEL Homestake site.
- Upgrades to the existing NuMI beam-line.

The relevant proton beam parameters are listed in Table 7.1.

Proton Beam Parameter	**Comment**
120 GeV beam energy	yields 2.3 MW beam power
1.7e14 Protons on target / spill	
1.4 second repetition rate	
10 microsecond spill length	Single turn extraction
2.4e21 Protons on target / year	Based on 2e7 seconds per year full power
25 pi-mm-mrad 95% transverse emittance from Main Injector (M.I.)	Estimate of what will be delivered by M.I.
momentum spread from Main Injector: 95% half spread at extraction to be smaller than 8E-4	Estimate of what will be delivered by M.I.
1.5 mm RMS beam spot size on target	Required by target design
~0.1 mm rms proton beam jitter on target	Driven by experimental systematics

Table 7.1 Proton beam parameters used for this study.

7.1 New neutrino beam-line to DUSEL

A selection by the NSF of the Homestake Mine site in Lead, South Dakota as the location for a future DUSEL site has motivated the consideration of the possible siting of a new Neutrino Production facility based upon protons extracted from the Main Injector. As sketched in Figure 1, it is possible to use the existing extraction system from the Main Injector for the Soudan, Minnesota based NuMI line as the front end for a new facility on the Homestake alignment. Just downstream of the existing "Carrier Tunnel" a new excavation can begin turning further to the west, and adjusting to the correct downslope to Homestake (5.84 degrees). A new Target Hall sized for the higher power available from the superconducting 8 GeV Linac will produce the mesons focused into a larger diameter decay pipe (4 to 5 meter diameter). About 400 meters of decay pipe is probably sufficient given the energy spectrum required for the neutrinos; 560 meters is shown in the figure. An absorber, and "Near Detector Hall" is then assumed and shown. This all fits on (under) the existing Fermilab site and most of the new excavation is either in the same rock strata already successfully mined for the NuMI excavation or in the upper "Galena" group.

Table 7.2 summarizes the top issues related to building a new neutrino beam line that could handle 2.3 MW of proton beam power. We find no target hall / beam line show-stoppers.

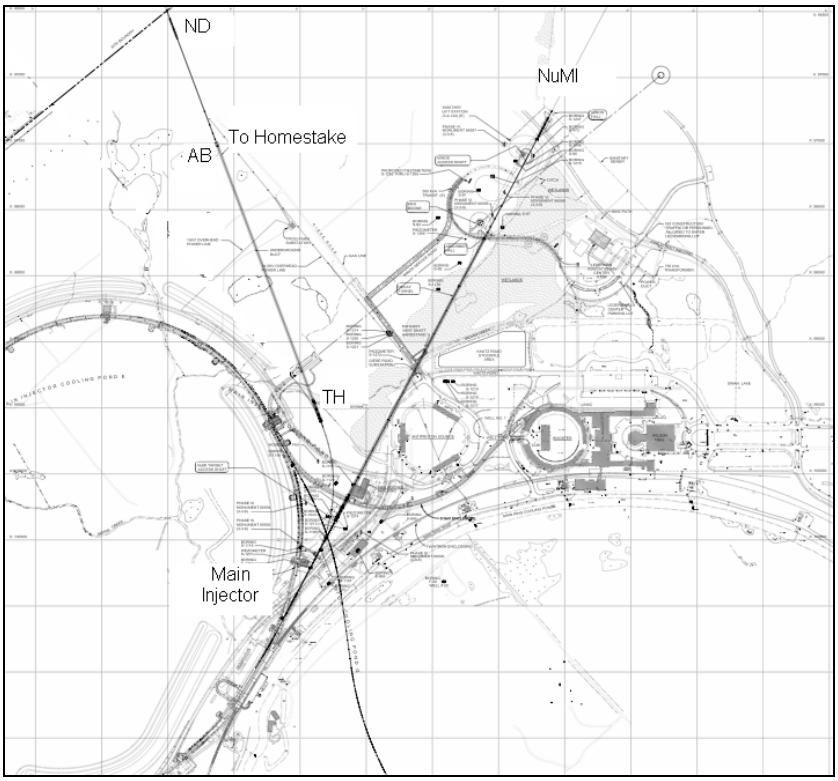

Figure 7.1 Beam-line layout to Homestake DUSEL site, showing target hall (TH), absorber (AB), and near detector (ND) locations with 560 m long decay region.

Issues considered for DUSEL beam-line	**Conclusion / Comment**
Would a new beam-line directed toward DUSEL fit on the FNAL site?	Yes (see Figure 7.1), including transfer line, target hall, decay pipe, absorber, rock for muon range-out and near detector.
Is there a target design that can survive these beam parameters?	Yes[37] Target stresses are OK for a graphite target (graphite is currently used for the NuMI target); some development is needed for design of cooling.
Can a beam window survive? (Transition from accelerator transfer line vacuum to target hall)	Yes, based on scaling energy deposition density per spill by spot size from existing AP0 Beryllium window. May have to add active cooling to the window.
Would existing section of transfer line have acceptable radiation loss with given emittance and momentum spread?	Yes, estimated emittance and momentum spread are consistent with existing transport line design.
Are there any other target hall / decay pipe / absorber issues that are technology limited?	None of the other components push the limits of current technology.

Table 7.2 Issues considered for neutrino beam-line to DUSEL.

7.2 Upgrading the existing NuMI facility

Plans are well developed as part of the NoVA project to upgrade the existing NuMI beam-line from its original design for 0.4 MW beam to 0.7 MW beam. Preliminary studies have also been carried out for upgrades to 1.2 MW as part of the SNUMI proposal, and those upgrades appear quite doable. We have now looked at several issues (see Table 7.3) related to further increasing the beam power to 2.3 MW.

Some components of the existing NuMI facility cannot be upgraded in an economically reasonable fashion because they are already highly radioactivated and are not designed for remote handling. These components may limit operation to less than 2.3 MW. Further engineering studies are required to refine the limits. The studies so far indicate the limiting issue is stress between the steel decay pipe and the concrete shielding cast around it, with the resulting limit being about 2.0 MW[38]. The engineering code requires a larger safety factor because the decay pipe is a vacuum vessel. One way around this is to fill the decay pipe with 1 atmosphere of helium, which because the decay pipe would no longer be a vacuum vessel would allow us to operate closer to the actual calculated failure stress point, and thus at higher power (2.3 MW). A further advantage of a helium fill would be that by reducing the stress on the aluminum decay pipe window, it would allay concerns about possible corrosion of the window. Based on previous studies for the MINOS experiment[39], the additional helium would reduce neutrino flux by a few percent. Comments about other critical systems are included in Table 7.3.

One reason that it is possible to think of using a decay pipe and absorber meant for 0.4 MW of beam for the case of 2 MW beam is that the original systems were built with redundancy (extra cooling lines) and safety factors. A concern operationally is that we would now be using that redundancy / safety factor for base operations. For instance, if a water line fails during 2 MW operation, one will need to figure out a way to repair the water line rather than being able to just turn it off and keep running. A risk analysis should be done, but is beyond the current study.

A list of NuMI systems that will or may need to be upgraded to take the higher power beam are listed in Table 7.4.

Issue possibly limiting NuMI beam power	**Conclusion / Comment**
Ground water activation	Calculations indicate groundwater activation limits will not be exceeded by the projected number of protons per year[40]
Radioactive Air Emissions	Calculations indicate that radioactive air emissions would be just below regulatory limits.[40] Alterations such as slowing down the ventilation fans would provide a safety factor.
Decay Pipe Window	(i) Calculations indicate that an accident pulse which missed the target and reached the window would be problematic. This can be mitigated by having the baffle upstream of the target completely occlude the area where beam would miss the target. (ii) Although direct radiation damage to the window is not expected to be problematic, accelerated corrosion due to the high radiation environment is a concern. This concern could be ameliorated by filling the decay pipe with 1 atmosphere of helium, thus reducing the stress on the window.
Decay Pipe	Stress due to thermal expansion may limit operation to 2.0 MW beam power.[38]
Hadron Absorber	(i) Calculations indicate the absorber can handle normal operating conditions with 2.3 MW beam.[38] (ii) An accident condition where beam mis-steered off the target would hit the absorber can be prevented by changing the upstream target / baffle geometry. (iii) An accident condition where cooling water flow fails requires further study, and may necessitate mitigation. The pipes carrying water to the aluminum core of the absorber pass through holes in the downstream steel slabs of the absorber. With 2.3 MW beam power, the innermost steel slab will reach 800 C. The concern is that without water flowing, the heat from the steel slab may damage the water pipe. [38]
Residual Dose in work area above chase and in Absorber cave	Dose rate can be mitigated with additional shielding.[40]
General degradation of components and infrastructure (accelerated corrosion and radiation damage).	Direct radiation damage will not be limiting (although extra shielding for electronics in the target hall is needed). Accelerated corrosion is hard to quantify, and further study/experience is needed.

Table 7.3 Issues with potential to limit beam power that could be accepted by an upgraded NuMI beam-line.

NuMI components to be upgraded	Comment
Target	Preliminary design is described in *NuMI Note 1100*, IHEP Protvino, July 30, 2005[41]
Horns	The outer conductor of each horn will require increased water cooling.
Hadron Monitor	Existing monitor would saturate; need smaller ionization gap
Beam profile monitor ?	Could certainly use the existing monitors if we drive them out of the beam for high intensity running, so did not examine this issue further
Cooling of beam pipe window	Forced air on face or water at edge
Target pile cooling	Have explored the concept of water-cooled panels lining inner walls of steel shielding
Decay pipe cooling	Increase water flow rate
Absorber cooling	Handle case of water steaming at steel penetrations if pumps fail
RAW skids	Increase heat exchanger capacities
Cooling pond	May exceed capacity of existing cooling ponds, or want to evaporate tritium for ALARA (further study needed)
Equipment to handle and transport radioactivated horns and target	May want to dig a new side-tunnel for storage of broken horns. Will need increased shielding when working on horns and target.
Refurbishment or replacement of crane rails, target hall drip ceiling, etc.	Depends on corrosion rate and deterioration seen.
Horn and target support modules	Depending on corrosion seen, may build replacement modules.
Equipment for further air containment	Allow more time for decay of short-lived radionuclides in the air
Further shielding for electronics located inside the target hall	Increase thickness of exiting poly shielding

Table 7.4 Components of the NuMI beam-line that would/may require upgrading for the higher beam power.

8 References

[1] http://protondriver.fnal.gov/SCRF_PD_v56.doc
[2] http://www-bd.fnal.gov/pdriver/H-workshop/hminus.html
[3] http://www-bd.fnal.gov/pdriver/H-workshop/chou_4_conclusions.pdf
[4] http://protondriver.fnal.gov/#Technical_Design_Link
[5] http://www.fnal.gov/directorate/DirReviews/Dir%27sRev_TechnicalReviewoftheProtonDriver_0315.html
[6] D.E. Johnson, Design of an 8 GeV H- Transport and Multi-turn Injection System, Proceedings of LINAC 2006, Knoxville, Tenn., p.779.
[7] N. Catalan-Lasheras and D. Raparia, The Collimation System of the SNS Transfer Lines, Proceedings of PAC 2001, Chicago, Ill, p. 3263.
[8] W. Chou, et. al., 8 GeV H- Ions: Transport and Injection, Fermilab-Conf-05-225-AD
[9] H.C. Bryant, Photodetachment of H- by Cavity Radiation Update, http://www-bd.fnal.gov/pdriver/H-workshop/bryant.pdf
[10] Tom Nicol, Private communication, March 16, 2006.
[11] J.P. Carneiro,Start-to-End Simulations for the Proposed Fermilab High Intensity Proton Source, proceedings of PAC 2007, Albuquerque, NM, TUPAS012, p. 1676.
[12] D. Johnson, Modifications to the Main Injector Lattice to Create a Symmetric Straight Section for H- Injection, Beams-doc 2363-v1, sept. 2006.
[13] A. Drozhdin, et. al. program STRUCT user manual, http://www-ap.fnal.gov/users/drozhdin/STRUCT/
[14] Steve Hays, private communication.
[15] Sarah Cousineau, SNS, private communication.
[16] D.E. Johnson, et.al., An 8 GeV H- Multi-turn Injection System for the Fermilab Main Injector, proceedings of PAC 2007, Albuquerque, NM, TUPAS020, p. 1700.
[17] Stefan Zeisler, TRIUMF, private communication.
[18] Martin Hu, Recycler electronic log book entry, Feb, 1, 2007.
[19] D.E. Johnson, et. al., A Conceptual Design of an Internal Injection Absorber ofr 8 GeV H- Injection into the Fermilab Main Injector, proceedings of PAC 2007, Albuquerque, NM, TUPAS018, p. 1694.
[20] D.E. Johnson, et al., "An 8 GeV H- Multi-Turn Injection System for the Fermilab Main Injector", in Proceedings of PAC-2007, Albuquerque, 2007, TUPAS020
[21] J.T. Volk, "Summary of Radiation Damage Studies on Rare Earth Permanent Magnets", http://home.fnal.gov/~volk/rad_damage/summary%20of%20radiation%20damage%20studies%20on%20rare%20earth%20permanent%20mangets.pdf
[22] A. Temnykh, "Measurement of Permanent Magnet Demagnetization due to Irradiation by High Energy Electrons", in Proceedings of PAC-2007, Albuquerque, 2007, TUPMS023
[23] 'Status of the Main Injector and Recycler,' S.D. Holmes, ", in Proceedings of PAC-2005, Oak Ridge National Laboratory.
[24] Type 8 Strontium Ferrite data sheets & specifications from Hitachi, Edmore, MI.
[25] D. Johnson, et.al., "An 8 GeV H^- multi-turn injection system for the Fermilab Main Injector, PAC-2007.
[26] W. Chou, et. al., "Design of a gamma-t-Jump System for Fermilab Main Injector", PAC-1997, Vancouver, Canada.
[27] C. Ankenbrandt, et. al., "Delivering Protons to the Antiproton Source After the Tevatron Collider Era", Beams-doc 2678 v1. , March 2007.
[28] D. Johnson, "Modifications to Main Injector Lattice to Create a Symmetric Straight Section for H- Injection", Beams-doc 2363 v1, September 2006.
[29] J. Johnstone, "A Simplified Analysis of Resonant Extraction at the Main Injector", Beams-doc 092 v2, September 1993.
[30] J. Johnstone, private communication.
[31] D. Wildman, private communication
[32] E.G.Cook, et.al. "Solid-State Modulators for RF and Fast Kickers", Proceedings of PAC2005, Knoxville, TN., p637.
[33] C. Ankenbrandt, et. al., "Using an ILC-Style 8 GeV H- Linac for a Muon to Electron Conversion Experiment", Beams-doc 2812 v1, July 2007.
[34] D. McGinnis, "A 2-megaWatt Multi-Stage Proton Accumulator", beams-doc 1782 v7, November 2005.

[35] D. Neuffer, "Rebunching in the Debuncher for m-e Conversion Experiments" Beams-doc 2501 v1, October 2006.
[36] D. Neuffer, "More Rebunching Options for the m2e Conversion Experiments", Beams-doc 2787 v1, May 2007.
[37] NuMI Note 1100, IHEP Protvino, July 30, 2005
[38] Beams-doc-2845, Bob Wands
[39] NuMI-note 777
[40] Beams-doc-2844, Kamran Vaziri
[41] NuMI Note 1100, IHEP Protvino, July 30, 2005